frontiers
in Chemistry

Check for updates

Nanoscale Metal–Organic Frameworks and Their Nanomedicine Applications

Dan Zhao[1]*, Wang Zhang[1], Zhi-Han Wu[1] and Hui Xu[1,2]*

[1]School of Marine Sciences, Ningbo University, Ningbo, China, [2]College of Plant Protection, Northwest A&F University, Yangling, China

Abundant connectivity among organic ligands and inorganic metal ions makes the physical and chemical characters of metal-organic frameworks (MOFs) could be precisely devised and modulated for specific applications. Especially nanoscale MOFs (NMOFs), a unique family of hybrid nanomaterials, with merits of holding the nature as the mainstay MOFs and demonstrating particle size in nanoscale range which enable them prospect platform in clinic. Adjustability of composition and structure allows NMOFs with different constituents, shapes, and characteristics. Oriented frameworks and highly porous provide enough space for packing therapeutic cargoes and various imaging agents efficiently. Moreover, the relatively labile metal-ligand bonds make NMOFs biodegradable in nature. So far, as a significant class of biomedically relevant nanomaterials, NMOFs have been explored as drug carriers, therapeutic preparation, and biosensing and imaging preparation owing to their high porosity, multifunctionality, and biocompatibility. This review provides up-to-date developments of NMOFs in biomedical applications with emphasis on size control, synthetic approaches, and surfaces functionalization as well as stability, degradation, and toxicity. The outlooks and several crucial issues of this area are also discussed, with the expectation that it may help arouse widespread attention on exploring NMOFs in potential clinical applications.

Keywords: nanoscale MOFs, drug carriers, nanomedicine, biosensing and imaging, therapeutic preparation

INTRODUCTION

During the past 2 decades, the merging of nanotechnology and medicine has confirmed the biomedical behaviour of a series of nanomaterials and improved some of them effectively in clinic (Banerjee et al., 2020). A large number of nanomaterials have been obtained with expansive dimension scope from several nanometers to hundreds of nanometers, and the great majority of these nanomaterials have exhibited bright prospects in clinic, for example drug delivery, photodynamic therapy, thermal therapy, chemotherapy, and biomedical sensing and imaging (Coughlan et al., 2017; Yang B et al., 2019; Mir et al., 2020; Wen et al., 2021).

As a burgeoning and fascinating stream of organic–inorganic hybrid materials, Metal-organic frameworks (MOFs) are consist of inorganic metal ions/clusters and multipoint organic bridging linkers (Li S Y et al., 2017). In light of the diversity of the connections among organic linkers and metal ions, the physical and chemical characters of MOFs could be rationally controlled and regulated for particular applications, especially when minimizing the size to nanoscale regime make it a foreground platform in biomedicine (Lismont et al., 2017;
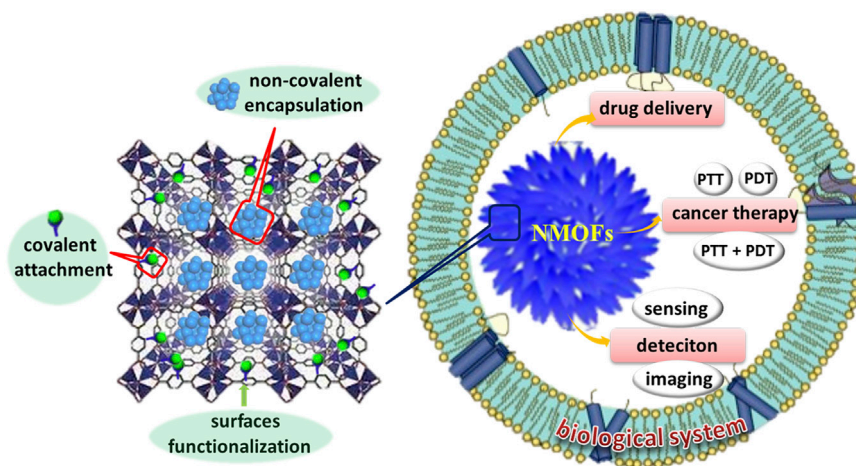
**FIGURE 1 |** Schematic diagrams of NMOFs in biomedicine.

Wu and Yang, 2017). Nanoscale MOFs (NMOFs) stand for a special class of hybrid nanomaterials. The merits of sustaining the properties and structural various as bulk MOFs and maintaining the size at the nanometer level let NMOFs perfectly capable applying in biomedical sciences (Lu et al., 2018a; Zhou et al., 2018; Bieniek et al., 2020; Li et al., 2020). Moreover, Compared with existing nanocarriers, NMOFs possess several potential advantages which make them have a wider application prospect for biomedicine: 1) structural and compositional adjustability permitting to build NMOFs owning diverse constitution, shapes, and characteristics; 2) oriented frameworks and high porosity provide enough space for lade therapeutic agents and various imaging efficiency; and 3) weaker coordination bond make them easily to be biodegraded.

In this review, the main focus is to highlight the recent research progress of NMOFs in the biological area, including the development of NMOFs in targeted drug delivery and cancer therapy, biomedical sensing and imaging as well as the toxicity, degradation, and stability of this class of novel hybrid nanomaterials (**Figure 1**). First, the general strategies to functionalize NMOFs for biomedicine-available considerations are briefly summarized, including pore encapsulation, and surfaces functionalization. Then, recent biomedical applications of NMOFs are discussed, including NMOFs as nanocarriers for intracellular delivery of drugs; as phototherapeutic agents for cancer therapy; and as fluorescent probes for biomedical sensing and imaging. Additionally, the outlooks and several crucial issues of this area are also mentioned with the expectation of stimulating more attention on investigating the potential of NMOFs for clinical applications.

NANOSCALE METAL–ORGANIC FRAMEWORKS

Nanoscale metal-organic frameworks (NMOFs), a peculiar class of metal-organic self-assembly materials, integrate the

merits of beneficial property of bulk MOFs and nanomaterials. First, highly porous and large channels enable NMOFs loading imaging agents and/or therapeutic preparations efficiently meanwhile by covalent attachment the construction units—whether metal ions/cluster or organic ligands—both can be used to payload imaging cargoes and/or drugs (Chen D et al., 2017; Hang et al., 2017; Yin et al., 2017; Cao et al., 2021). For example, by choosing construction units or decorating imaging components, NMOFs-based diagnostic and therapeutic agents have been extensively developed and used for magnetic resonance imaging (MRI) (Chowdhuri et al., 2016), computed tomography (CT) (Tian et al., 2015), positron emission tomography (PET) (Zhao et al., 2016a), and optical imaging (Yang S P et al., 2017). Second, appropriate selection and functionalization of organic linkers and building blocks allows NMOFs to load and release imaging agents and drugs components in steerable patterns both spatially and temporally, emphasizing their latent roles on theranostic platforms (Ni et al., 2020a). The inorganic metal components on NMOFs also make them attractive contrast medium for biomedical optical applications. So far, therapeutic construction units have been encapsulated into NMOFs for particular treatment. Such as, using photosensitizers as construction groups permit the NMOFs effective for photodynamic therapy (PDT), meanwhile, high-Z metal ions-containing NMOFs materials possess excellent X-ray attenuation ability could be used as radiosensitizer to improve field radiotherapy (RT) (Nazari et al., 2016). Third, the adjustable skeleton stability of NMOFs in physical surroundings permits to obtain activated or controlled-release nanocarriers. Additionally, many sorts of NMOFs have been certificated with low cytotoxicity ensures them applications *in vivo*. Also, in light of the comparatively weaker metal-ligand coordinate bonds, the NMOFs are biodegradable in nature (Morris et al., 2017). These exceptional merits of the NMOFs make them a promising platform for biomedical field.
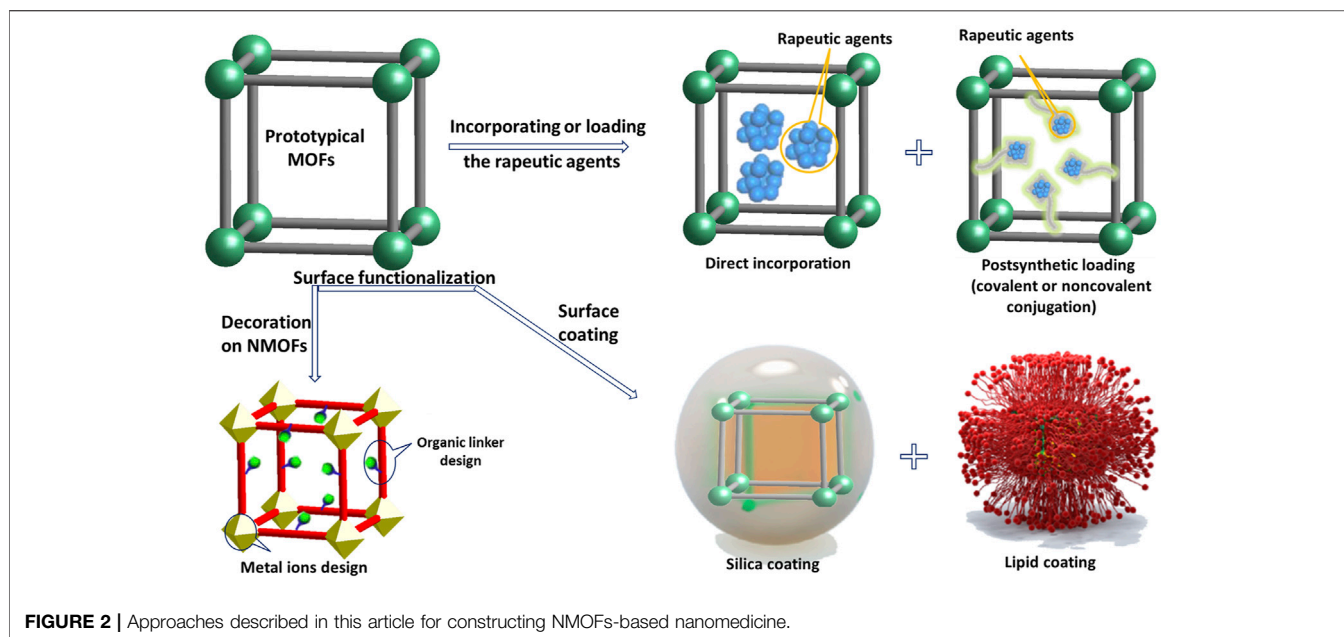
FIGURE 2 | Approaches described in this article for constructing NMOFs-based nanomedicine.

Synthesis and Design Strategies of Nanoscale Metal–Organic Frameworks-Based Nanomedicine

For biomedical applications, the first attention should be paid to scaling down particle size within nanoscale (Cai M et al., 2020). As porous nanomaterials, NMOFs could be designed with a limitless array of inorganic and organic components. Normally, to acquire nanoscale MOFs, two factors should be considered: 1) limiting the supramolecular assembly; a process that usually results in the formation at nanoscopic locations and 2) supporting nucleation against crystal growth. Currently in literature, controlled synthetic techniques of NMOFs gradually have been divided into four categories: nanoprecipitation, solvothermal synthesis, surfactant-assisted approach, and reverse microemulsion method (Rieter et al., 2008; Liu et al., 2012; Baa et al., 2019). In these methods, reactant ratio, temperature, pH, reaction conditions, etc. factors affect the growth and nucleation of NMOFs during the synthetic progress (Zhao et al., 2018). NMOFs occupy various merits over traditional nanomedicines for example their structural diversity, their loading capacity, and their biodegradability. A great deal of NMOFs has been certified as bioimaging agents both *in vivo* and *in vitro* (Cai et al., 2015). Researchers have used two general approaches to construct NMOFs-based nanomedicine, as shown in **Figure 2**: one is incorporating active groups into the skeleton or loading active agents into the channels and pores of the NMOFs; the other one is surface modification of as-synthesized NMOF by silica coatings or organic polymers to improve their stabilities, slightly regulated their physicochemical characteristics, and afford extra functionality and biocompatibility. For pore encapsulation strategy: NMOFs as a host material can prevent the loaded substrates from leaching, as well as providing them a protective environment against external

adverse factors. Surfaces functionalization strategy for NMOFs can meet the specific requirements and acquire the expected function, which is extremely significant in clinic. However, these two strategies require that NMOFs and the substrate are stable under synthetic conditions.

Incorporating or loading the rapeutic agents within NMOFs: Molecular nature of NMOFs can give materials various characters. The moderate synthetic conditions and tunable components of NMOFs allow for the capacity of therapeutic and imaging agents while at the same time guaranteeing effective delivery to internal specific cells (Simon-Yarza et al., 2018). Generally, there are two general categories for cargo loading in NMOFs: incorporating cargoes directly during particle synthesis and postsynthetic loading. Additionally, complementary of these two strategies can also be applied for merging multiple biomedically relevant groups and NMOFs to develop theranostic agents.

In the method of direct incorporation, bioactive agents (the metal notes or the linkers) can be incorporated within NMOFs directly during their self-assembling process. The most commonly used therapeutic preparations based-MOFs are generally have fairly good stability in water solution such as Zr-MOF (Abánades Lázaro et al., 2020), porphyrinic MOF (Li et al., 2021), zeolitic imidazolate frameworks (ZIF) (Pan et al., 2017), and Fe-MOF (Cui et al., 2021). Although extremely high agents loading with equidistribution could be achieved by direct incorporation method, but the physic-chemical characters and morphology of these materials require to be adjusted separately. Apart from being incorporated directly, biomedically relevant units can also be imported within NMOFs in the synthesis process by object encapsulation. Various agents with different properties have been used to encapsulate into NMOFs by this strategy for example proteins, small particles, dyes, and drugs [35]. But, this method can only achieve a lower drug loading, and that

the release kinetics of the drug from the NMOF and the skeleton decomposition rate may be extraordinary different.

Postsynthetic loading is another loading method for encapsulating biomedically relevant molecules within NMOFs. After obtaining highly porous NMOFs with specific physiochemical properties, the active units are then packed into the NMOFs via covalent or noncovalent surface conjugation. Covalent postsynthetic modification is realized by functional groups in NMOFs react with bioactive reagents (Nguyen et al., 2010). As a case, a BDC-NH$_2$ (2-amino terephthalic acid) group including NMOFs has been used to link contrast medium and chemotherapeutic agents via covalent conjugation (Huang et al., 2006). Noncovalent surface conjugation offers another effective way for loading drugs and an extraordinary load amount with 1.4 g of ibuprofen/g was achieved in MOF-101 (Horcajada et al., 2006).

Surfaces functionalization of NMOFs: Surfaces functionalization of NMOFs to meet the specific requirements and acquire the expected function is extremely significant in clinic. The controlled manipulation of the external surface of NMOFs improves the water dispersibility, reduces nonspecific binding with plasma protein, and appends other components to specific areas or to add extra functionalities or groups (Horcajada et al., 2006; Alexis et al., 2008).

Since NMOFs are formed by ligands and ions, the primary task is to decorate a connector on ligands before MOF assembly and then covalently bonding the specific agent with the connector on the superficies of the as-synthesis NMOFs (Zhu et al., 2018). For example, as the organic ligand in UiO-66, 1,4-benzenedicarboxylic acid without connector lead to the resultant UiO-66 cannot be functionalized by covalent modification. Conversely, 2-azido terephthalic acid, the organic linkers of UiO-66-N$_3$, where the azide group could react with the alkane group by click reactions to modify the desired agent on the surface of MOF. Finally, a dibenzylcyclooctyne terminal DNA sequence sucessful bonded with the surface of UiO-66-N$_3$ without any internal change in the whole chemical transformation process (Morris et al., 2014). The second strategy is using the chelating ability of metal ions and target molecule to connect the specific agents on the MOF surface directly (Wang et al., 2017; Wang et al., 2019). Surface defects of NMOFs, such as the unsaturated coordinative metal sites (CUS), give NMOFs the ability to combine with target molecules by coordination. At present, different functional group-terminal ligands have been incorporated to NMOFs by coordinating to the metal-sites through external secondary modification including phosphonate, carboxylate, phenyl, and histidine groups. For example, both phosphonate and carboxylate groups can bonding with Zr ions in Zr-based MOFs, thus decorating the surface of the Zr-based MOF with terminal phosphate-modified DNA successfully (Röder et al., 2017). His-tags can be easily fabricated in peptides or proteins greatly expanding the range of targeted molecule-functionalized MOFs. Phenolic capped linkers also can generate the coordination bonds to modify MOF a stable material via post-synthetic (covalent) modification (Wang et al., 2015). A great variety of ions have been certified to be able to chelate with phenolic units to afford stable 5-member ring including Fe, Zr, Cr, Cu, Zn, Co, In, Eu, and Al.

Surface coating provides another convenient way to modify NMOFs with their structural integrity and porosity unchanged. During surface coating process, some factors should be considered: 1) biofriendly synthesise without any poisonous substance; 2) prevent the targeting molecule invading into the nanocarrier; 3) reduce interference with entrapped drugs; 4) keep drug release capacity; 5) improve the stability of particle colloidal, and 6) stable under physiological environment. So far, silica coating and lipid coatings have been considered the most effective strategies for NMOFs surface coating, especially for stabilizing physiologically unstable NMOFs. For promoting process of the silica coating, firstly the surface of NMOFs is decorated with a polymer, like polyvinylpyrrolidone (PVP). For instance, Lin and co-workers have obtained a series of NMOFs by silica coating (Rieter et al., 2008). Authors represented an universal way to acquire different silica shells thickness on the surface of Ln(BDC)$_{1.5}$(H$_2$O)$_2$ (Ln = Gd^{3+}, Eu^{3+}, or Tb^{3+}, BDC^{2-} = 1,4-benzenedicarboxylate); Tb$_2$(DSCP)$_3$(H$_2$O)$_{12}$ (DSCP = c,c,t-(diamminedichlorodisuccinato), Mn$_3$(BTC)$_2$(H$_2$O)$_6$ (BTC^{3-} = 1,3,5-trimesic acid), and Cr$_3$F(H$_2$O)$_2$O(BDC)$_3 \cdot n$H$_2$O (where n is ~25). Eventually, they loaded dipicolinic acid (DPA), Pt-based drugs, acyclicarginine-glycine-aspartate (RGD) peptide, and optical imaging contrast agent (BODIPY) into nanoscale materials stabilized with silica shell for biological application. Although silica coating method seems to be a widespread approach for various materials, it is hard to gain flimsy silica shells. Furthermore, weakly basic coating condition is incompatible with material. Lipid coating is not only available for slowing down the kinetics of releasing cargos but also efficient for imparting biocompatibility (Wuttke et al., 2015). The Mirkin group used the lipid ligand 1,2-dioleoyl-snglycero-3-phosphate (DOPA) to transfer a family of Zr^{IV}-based NMOFs facilely be dispersed and suspended in solvents with low polarity by easily surface encapsulation. Differ from artificial lipid layers, exosomes which have membrane structures similar with cell membranes, are usually used by cells for communication purposes. The Wuttke and co-workers coated exosomes on MIL-88A surface successfully to investigate the sustained-release of calcein in HeLa cells (Illes et al., 2017). Although a significant progress have been achieved in NMOFs modification, there are still unsolved problems in aspect of concrete characterization of targeting/coating stability and efficiency (Meng et al., 2016; Abánades Lázaro et al., 2017). In addition, for fulfilled potential of NMOF-based therapeutic and imaging agents, rigorous *in vivo* and *in vitro* researches are acquired.

NANOMEDICINE APPLICATIONS OF NANOSCALE METAL–ORGANIC FRAMEWORKS

Unique molecular architecture and versatile functionalities make NMOFs potential platforms for drug delivery, cancer therapy, biomedical sensing, and imaging applications (Velásquez-Hernández et al., 2020). In this section, the parameters of

NMOFs before the biomedical applications of NMOFs will be discussed and the recent research progress related to nanomedicine applications of NMOFs in clinical is summarized in the context of translational medical research.

Parameters of Nanoscale Metal–Organic Frameworks in Biomedicine

Although most NMOFs have the characteristics of high surface areas, tunable pore size, crystallinity, thermal stability, and so on, but for medical applications, some strict parameters should be considered (McKinlay et al., 2010). Once MOFs are utilized in biologically and medical applications, characteristics like stability, biodegradability, and toxicity need to be addressed further.

Stability: Before the successful applications of NMOFs in diagnosis and treatment, the stability in the physiological surrounding of NMOFs should be discussed. By scanning electron microscope (SEM), high-resolution transmission electronic microscope (HRTEM), X-ray diffraction (XRD), and other experimental characterization methods, the stability of NMOFs in water solution, buffer solution, and different pH conditions could be evaluated. Although few NMOFs are obtained from the aqueous phase, most of them are still stable in the aqueous solution, including UiO MOF series, PCN MOF series, Ni-CPO-27, Cr-MIL-100, Cr-MIL-101, MIL-125, CAU-1, and ZIF-8 (Yang et al., 2011; Jeazet et al., 2012; Liu et al., 2015). Lin groups obtained a nanosensor on account of fluorescein isothiocyanate (FITC) conjugated UiO-68 (F-UiO) for pH sensing in cell (He et al., 2014a). The fluorescein FITC is pH sensitive and shows pH-dependent ratiometric fluorescence changes, certificating its ability to sense the pH_i in cells. F-UiO exhibited unaltered hexagonal plate morphology after incubating in Hank's Balanced Salt Solution (HBSS) for 24 h. Negligible FITC dye leaching experiment and XRD patterns indicate that the structural of F-UiO was stable in cell.

Degradation: Biodegradability of MOFs is another important issue that needs to be emphasized in term of biological application (Wu et al., 2018). By compared the release mechanism of drug in NMOFs with two other coating methods, Amorín-Ferré and co-workers found that NMOFs with a formula of [Co(bix)(3,5-dbsq)(3,5-dbcat)] (bix = 1,4-bis(imidazol-1-ylmethyl)benzene) could be designed in spherical structures with a diameter of 150–200 nm, where $3,5\text{-}dbsq^-$ and $3,5\text{-}dbcat^{2-}$ are respectively the semiquinonate radical and catecholate forms of 3,5-di-tert-butyl-1,2-benzoquinone (dbq) (Amorín-Ferré et al., 2013). Physical encapsulated drugs within NMOFs will be released by free diffusion, but covalently bound drugs within the structures can only be governed by slow particle degradation. Detailed description of this situation in the case of MIL-100(Fe) nano- or microparticles confirmed the gradual formation of dense forms in the process of degradation in a simulated physiological environment. Also, the excretion and degradation mechanism proved that the Fe-MOFs could be quickly segregated by organism and then eliminated and biodegraded safely.

Toxicity: For the ultimate biomedical goal of NMOFs in clinical, toxicity issues should be solved by a more reasonable safe-by-design approach. As MOFs consist of metal ions/cluster and organic linkers, some nontoxic or low-toxic inorganic metal ions and organic ligands should be selected to produce NMOFs for reducing of toxicity from the source. As kinds of essential microelements to human body, Cu, Zn, Fe, Mn, Mg and Zr metal ions, have been heavily applied in NMOFs assembly with acceptable toxicity decided by oral lethal dose 50 (LD50), i.e., 350 µg kg^{-1} for Zn, 25 g kg^{-1} for Cu, 30 g kg^{-1} for Fe, 4.1 g kg^{-1} for Zr, and 1.5 g kg^{-1} for Mn (Amorín-Ferré et al., 2013; Wu and Yang, 2017). As for exogenous organic linkers, terephthalic acid (LD50 = 5 g kg^{-1}), fumaric acid (LD50 = 10.7 g kg^{-1}), trimesic acid (LD50 = 8.4 g kg^{-1}), terephthalic acid (LD50 = 5 g kg^{-1}), 5-aminoisophthalic acid (LD50 = 1.6 g kg^{-1}), 2,6-napthalenedicarboxylic acid (LD50 = 5 g kg^{-1}), isonicotinic acid (LD50 = 5 g kg^{-1}), 1-methylimidazole (LD50 = 1.13 g kg^{-1}), and 2-methylimidazole (LD50 = 1.4 g kg^{-1}), are normally significant for bioapplications. Horcajada and co-workers did outstanding works on screening the general toxicity and cytotoxicity of a range of NMOFs in mice (Tamames-Tabar et al., 2014). In their experiment, three Fe-based NMOFs could be rapidly absorbed by mononuclear phagocytic system organs after intravenous injection. The Maspoch group systematically described *in vivo* toxicities of a series of NMOFs such as MIL-88A, MIL-88B-4CH$_3$, MIL-100, MIL-101, NOTT-100, HKUST-1, ZIF-7, ZIF-8, MOF-74 family (M = Ni, Co, Cu, Mg, Zn, and Mn), UiO-66, UiO-66-NH$_2$, UiO-67, and MOF-5 (Ruyra et al., 2015). The authors found that NMOF toxicity has a correlation with metal toxicity as well as particles shape/size.

Synthesis and Design Strategies of Nanoscale Metal–Organic Frameworks-Based Nanomedicine

Drug delivery have appeared as an important field of research due to the unacceptable fact is that traditional delivery patterns usually refer to large doses resulting in toxic side-effects by systemic circulation at unexpected targets (Li W et al., 2017). As efficient drug delivery vehicle, some requirements should be addressed, such as 1) controlled release the active agents; 2) maximum degradation and possibility to be surface modified by the delivery vehicle; 3) could be detected by diverse imaging techniques; 4) with high drug loading capacity; 5) toxicity and biocompatibility. The merits of diversified structural components and abundant performance make NMOFs have higher drugs loading ability, controlled release ability, and are easily modified by active agents (Al Haydar et al., 2017). Another aspect that has proved MOFs more attractive as drug delivery carriers is that a sole MOF can be applied to load multiple active agents as some of these materials exhibit a dual hydrophilic/hydrophobic pore structure. **Table 1** summarizes the drug release ability of various NMOFs as drug carriers. In NMOFs as carriers for targeted drug delivery system, two factors involve loading efficiency and stimulus-responsive drugs release should be discussed.

Loading efficiency: Thanks to their porous structure, NMOFs have a more drug loading efficiency compared to conventional materials. The loading agents can range from small molecules to
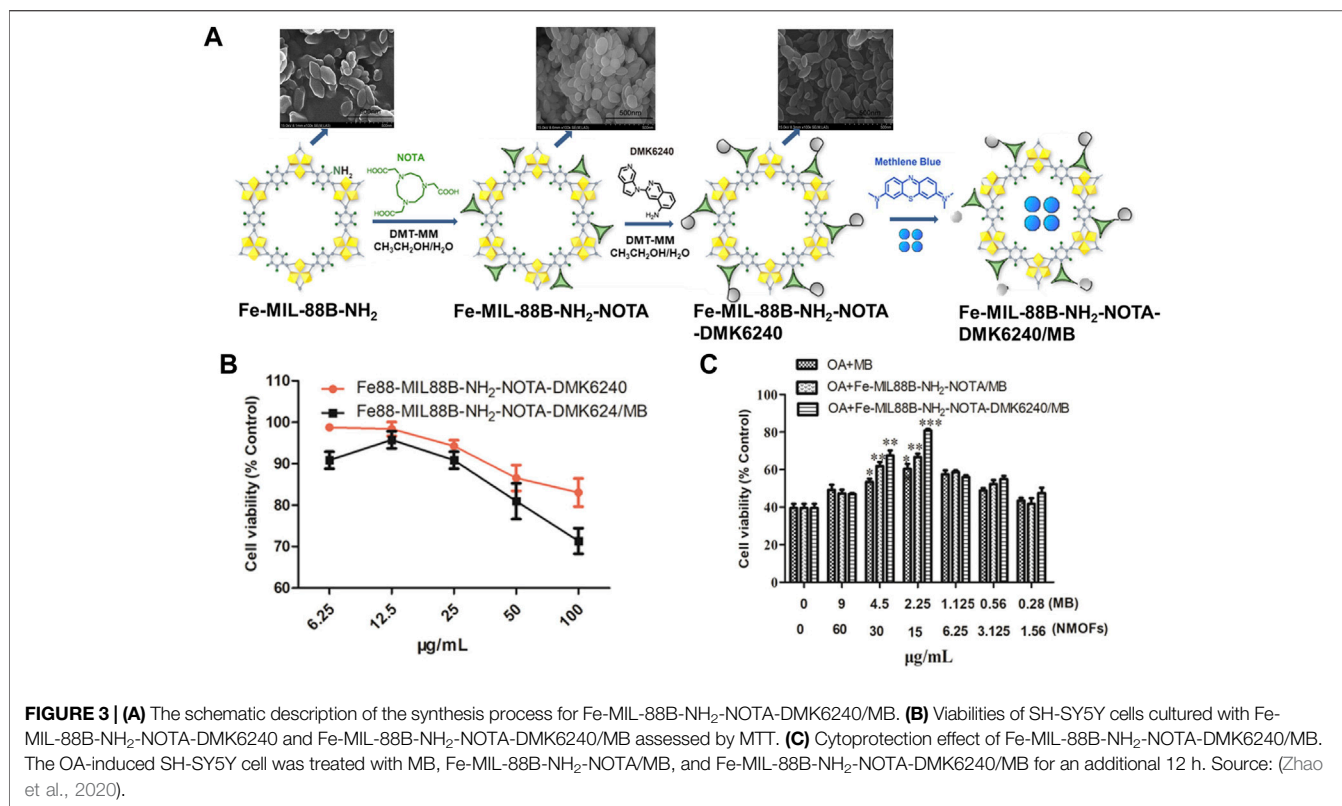
TABLE 1 | The drug release ability of various NMOFs as drug carriers.

NMOFs	Drugs	Drugs loading effective (wt%)	Ways to stimulate drug release	Refs
MIL-53	ATP-TP; Bu; CDV; Doxorubicin (doxo)	0.24 of AZT-TP, 14.3 of Bu	-	Horcajada et al. (2010)
MIL-88A		0.6 of AZT-TP, 8.0 of Bu, 2.6 of AZT-TP, 8.0 of CDV		
MIL-89		9.8 of Bu, 14 of CDV		
MIL-100		25 of Bu, 21 of AZT-TP, 16 of CDV, 29 of doxo		
MIL-100-NH$_3$		42 of AZT-TP, 41.9 of CDV		
UIO-MOFs	cisplatin	12	-	He et al. (2014a)
Se/Ru@MIL-101	siRNAs	13.93	-	Chen D et al. (2017)
Fe-MIL-88B-NH$_2$	1,4,7-triazacyclononane-1,4,7-triacetic acid (NOTA) 5-amino-3-(pyrrolo [2,3-c]pyridin-1-yl)isoquinoline (defluorinated MK6240, DMK6240) methylene blue (MB)	15 of MB	-	Zhao et al. (2020)
ZIF-8	DOX	15	pH	Zheng et al. (2016)
	3-MA	19.798	pH	Chen W H et al. (2018)
	glucose oxidase (GOx), insulin	15.6 of GOx, 52.3 of insulin	ROS, Glucose, pH	Lu K et al. (2016)
NU-1000	insulin	40	-	Chen W H et al. (2018)
NU-1000x (x = 3, 4, 5, 6, 7)	Lactate dehydrogenase (LDH)	-	-	Li P et al. (2018)
ZIF-90	Rhodamine B (RhB)	-	ATP-responsed	Deng et al. (2017)
	sgRNA), CRISPR/Cas9	-	ATP-responsed	Yang X et al. (2019)
ZJU-64	MTX	13.45	Temperature, pH	Lin et al. (2016)
ZJU-64-CH$_3$	MTX	10.63	Temperature, pH	Lin et al. (2016)
UIO-66-NH$_2$	5-fluorouracil (Fu)	-	Temperature, Zn^{2+}	Tian et al. (2015)
Bio-MOF-1	Procainamide	-	-	An et al. (2009)
MIL-101	BODIPY	5.6–11.6	-	Taylor-Pashow et al. (2009)
Zr-based-MOF	diclofenac sodium (DS)	58.80	Pressure, 37°C	Jiang et al. (2016)

proteins. Perfect NMOF therapeutic preparations typically have larger pore size and excellent aqueous stability, such as Zr-MOF series, ZIF series, porphyrinic MOF series, and Fe-MOF series larger pore size and excellent aqueous stability (Cai et al., 2019; He et al., 2019; Abánades Lázaro and Forgan, 2019; Cai X et al., 2020; Sun et al., 2020). Horcajada groups demonstrated a family of non-toxic iron (III) carboxylate NMOFs as degradable drug carriers to transport various drugs that are hard to deliver by other nanocarriers, such as MIL-53, MIL-88A, MIL-88Bt, MIL-89, MIL-100 and MIL-101-NH$_2$ (Horcajada et al., 2010). As drug carriers, their loading efficiency was detected by four commonly anticancer or antiviral drugs (azidothymidine triphosphate (AZT-TP), busulfan (Bu), cidofovir (CDV) and doxorubicin (doxo)), which, except the latter, could not be successfully encapsulanted using existing nanocarriers. The drug loading experiment showed that the NMOFs serve as a remarkable molecular 'sponges'. For example, up to 25, 21, 16 and 29 wt% of Bu, AZT-TP, CDV and doxo could be loaded into MIL-100. Moreover, a remarkable capacity of 42 wt% can be obtained for AZT-TP and CDV with MIL-101-NH$_2$.

Expect for single drug delivery, MOFs also can be serving as a nanocarrier for drug co-delivery to improve clinical effects. For example, Lin group successfully loaded siRNA and cisplatin together into UiO-NMOFs via encapsulation and surface coordination, respectively (He et al., 2014b). Cisplatin loading capability is up to 12 wt%. Later, Liu and co-workers decorated selenium (Se) and ruthenium (Ru) NPs and loaded siRNAs in the surface of MIL-101 successfully (Chen Q et al., 2017). The combination of Se/Ru-NMOFs and siRNA not only can significantly improve the therapy efficacy but also has high tumor-targeted, enhances antitumor efficacy, and reduces systemic toxicity *in vivo*. Recently, a multifunctional NMOF-based drug delivery system was obtained by Kong groups for targeting hyperphosphorylated tau (Zhao et al., 2020). As shown in **Figure 3A**, by post-synthetic modification of the surface of Fe-MIL88B-NH$_2$ with 1,4,7-triazacyclononane-1,4,7-triacetic acid (NOTA) and 5-amino-3-(pyrrolo [2,3-c]pyridin-1-yl) isoquinoline (defluorinated MK6240, DMK6240) and encapsulation of the tau protein aggregation inhibitor-methylene blue (MB), a drug system namely Fe-MIL-88B-NH$_2$-NOTA-DMK6240/MB was prepared successfully. The cytotoxicity of this drug system was evaluated in SH-SY5Y cells using the MTT method. The result demonstrates that almost 83% of SH-SY5Y cells were still alive 24 h of incubation with 100 μg/ml of Fe-MIL-88B-NH$_2$-NOTA-DMK6240 (**Figure 3B**). The 80% cell survival rate illustrates
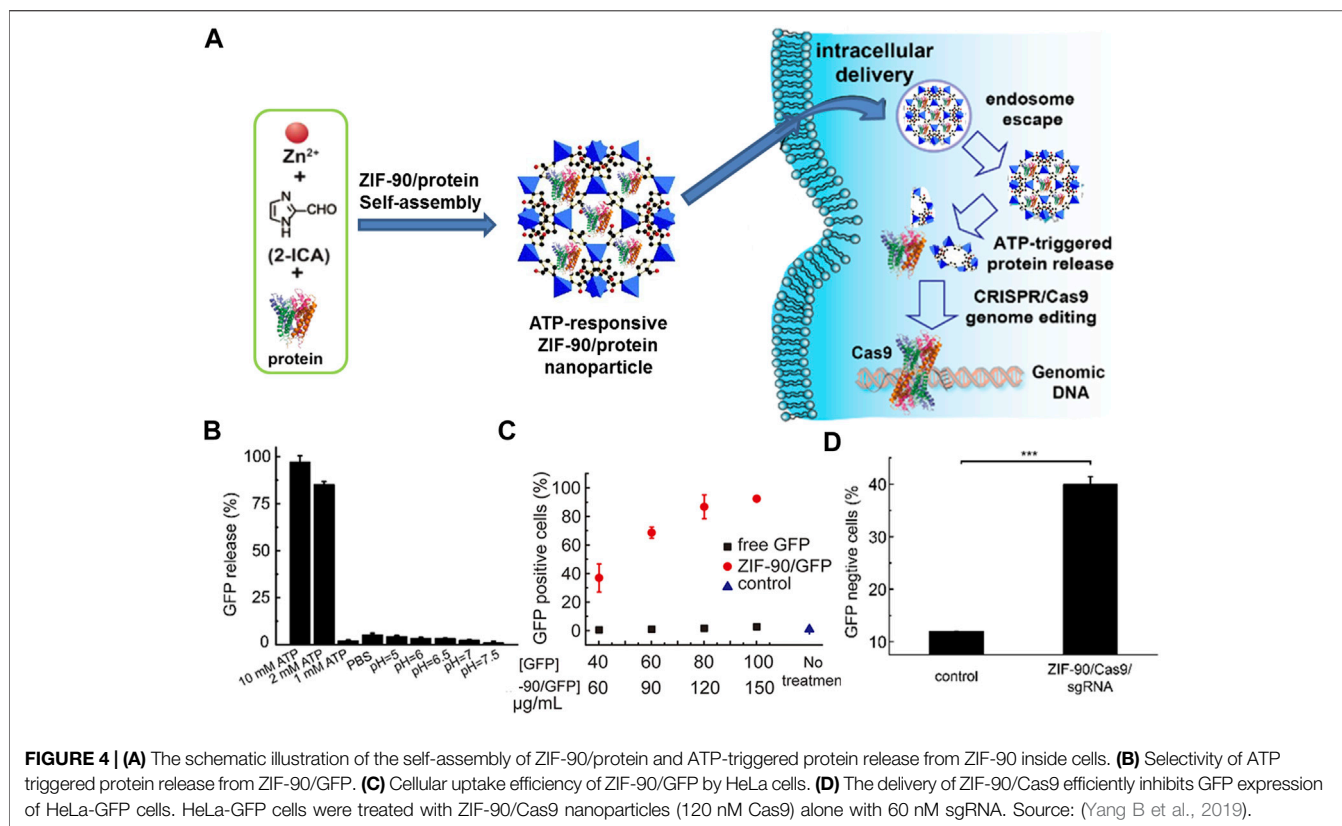
FIGURE 3 | (A) The schematic description of the synthesis process for Fe-MIL-88B-NH$_2$-NOTA-DMK6240/MB. **(B)** Viabilities of SH-SY5Y cells cultured with Fe-MIL-88B-NH$_2$-NOTA-DMK6240 and Fe-MIL-88B-NH$_2$-NOTA-DMK6240/MB assessed by MTT. **(C)** Cytoprotection effect of Fe-MIL-88B-NH$_2$-NOTA-DMK6240/MB. The OA-induced SH-SY5Y cell was treated with MB, Fe-MIL-88B-NH$_2$-NOTA/MB, and Fe-MIL-88B-NH$_2$-NOTA-DMK6240/MB for an additional 12 h. Source: (Zhao et al., 2020).

that Fe-MIL88B-NH$_2$-NOTA-DMK6240/MB can effectively protect neurons from death (**Figure 3C**).

In addition to improve the loading efficiency of NMOFs by multiple coordination between the active compound and metal sites, physisorption by soaking the as-synthesized NMOFs nanocarriers into drug-containing solutions is another method to improve load efficiency of NMOFs. For example, Zou groups combined the synthesis of ZIFs and the encapsulation of target organic molecules in one pot (Zheng et al., 2016). The anticancer drug doxorubicin (DOX) guest molecules which adsorbed into the frameworks of ZIF-8 nanoparticles could be targeted delivery efficient without premature release. Besides doxorubicin, an autophagy inhibitor 3-methyladenine (3-MA) also could be capped in ZIF-8 via one-pot synthesis (Chen W H et al., 2018). The experiment showed that a remarkable capacity of 19.798 wt% can be achieved for 3-MA with ZIF-8 nanoparticles.

Larger molecule delivery encounters more challenges because of their size, surface charge, and component effects including peptides and proteins (Kato et al., 2019). The protein loading efficiency could be significantly improved by immersing NMOFs with a bigger channel size into a protein-containing solution to do physical adsorption (Lian et al., 2017). Farha groups immobilized insulin in NU-1000 due to the larger one-dimensional pores of NU-1000 (mesopores with size ~30 Å and micropores with size~12 Å in diameters), and acquired a high loading of ~40 wt% in only 30 min (Chen X et al., 2018). The surplus insulin can be digested by pepsin and denatured by stomach acid. Conversely, when using NU-1000 as a nanocarrier for oral delivery of insulin, insulin@NU-1000 not only can keep the

wholeness of insulin in gastric acid but also can prevent pepsin from entering the insulin to limit proteolysis simultaneously. Subsequently, they expanded the pore apertures of a series of Zr-based MOFs (termed NU-1000x, x = 3, 4, 5, 6, 7) from 3.3 to 6.7 nm. The expanded NU-1000x MOF structures were used to incorporate the lactate dehydrogenase (LDH) and then demonstrated the use of the captured protein in a cell-free biosynthetic catalytic system (Li B et al., 2018).

Stimulus-responsive release: Although the terms of lower toxic, higher loading ability, and available organism permeability enable NMOFs as outstanding drug carriers, but the issues of premature drug release of NMOFs as nanocarrier is also extremely significant. Typically, stimuli-responsive factors of NMOFs are pH, biomolecules, temperature, and so on. Furthermore, loaded drugs of NMOFs could be activated by diverse stimuli (Lu K et al., 2016). For instance, acidic property of tumor tissue enables pH is one of the extensively studied stimuli for drug release. Willner and co-workers used ZIF-8 NMOF loaded glucose oxidase (GOx) and insulin, and the GOx-mediated aerobic oxidation of glucose yield H$_2$O$_2$ and gluconic acid (Chen Y et al., 2018). The high intracellular concentration of biomolecules in cell also can control drug release such as glutathione (GSH), adenosine triphosphate (ATP), and enzyme. Among numerous factors controlling drug release, disulfide bonds with GSH response is usually considered. Higher GSH level promote the reducing of the disulfide bond and finally set the drugs free. As an extremely important compound for organism, ATP usually used to offer energy and then promote biological processes deeper. Mao and

FIGURE 4 | (A) The schematic illustration of the self-assembly of ZIF-90/protein and ATP-triggered protein release from ZIF-90 inside cells. **(B)** Selectivity of ATP triggered protein release from ZIF-90/GFP. **(C)** Cellular uptake efficiency of ZIF-90/GFP by HeLa cells. **(D)** The delivery of ZIF-90/Cas9 efficiently inhibits GFP expression of HeLa-GFP cells. HeLa-GFP cells were treated with ZIF-90/Cas9 nanoparticles (120 nM Cas9) alone with 60 nM sgRNA. Source: (Yang B et al., 2019).

workers reported the first case of using nanoscale ZIF-90 to specific subcellular mitochondria and image dynamics of mitochondrial ATP in cells (Deng et al., 2017). After embedding Rhodamine B (RhB) in ZIF-90, RhB/ZIF-90 nanoprobe with fluorescence is able to monitor the ATP level fluctuation in a various scope of cellular processes. Later, ZIF-90 with ATP-responsive platform was developed by the same group to deliver cytosolic protein and clustered regularly interspaced short palindromic repeats-associated protein 9 (CRISPR/Cas9) genome editing, as shown in **Figure 4A** (Yang X et al., 2019). An interesting finder is a slower green fluorescent protein (GFP) release was observed when treated the ZIF-90/GFP in 10 mM phosphate-buffered saline, which is differ to ZIF-8-based protein release with pH-responsive (**Figure 4B**). Intracellular delivery studies indicated that the ZIF-90/protein nanocarriers can deliver abundant of proteins into the cytosol, regardless of protein size and molecular weight (**Figure 4C**). Because of the competitive coordination between ATP and Zn²⁺, the ZIF-90/protein nanocarriers decompose in the existence of ATP and release protein. Such as, compared with non-treated HeLa cells, ZIF-90/ protein treatment efficiently inhibited GFP expression in HeLa-GFP cells up to 40%, indicating an effective CRISPR/Cas9 genome editing upon ZIF-90/protein delivery (**Figure 4D**).

In general, release efficiency of drug molecules in temperature-responsive nanocarriers is more susceptible to temperature changes in living organisms. Sada groups reported an example of polymer-modified MOF tethering thermoresponsive polymer poly (N-isopropylacrylamide) (PNIPAM), showing thermally

ON-OFF controllable behavior (Nagata et al., 2015; Chen et al., 2019). Two Zinc-based MOFs with formula Zn_{16} (ad)$_8$ (TP)$_8$O$_2$(H$_2$O)$_4$·4HTP·36DMF·16H$_2$O (DMF = N,N-Dimethylformamide) were designed by Qian groups (ad = adenine, H$_2$TP = [1,1':4',1''-terphenyl]-4,4''-dicarboxylic acid for ZJU-64, and 2',5'-dimethyl-[1,1':4',1''-terphenyl]-4,4''-dicarboxylic acid for ZJU-64-CH$_3$) for loading anticancer drug methotrexate (MTX) (Lin et al., 2016). By an easy impregnation method, anticancer drug MTX could be incorporated into NMOFs and loading capacity of ZJU-64 is 13.45 wt%, of ZJU-64-CH$_3$ is 10.63 wt%. Furthermore, equal amounts of MTX drugs released from MTX-loaded ZJU-64 and ZJU-64-CH$_3$ at 37°C took 72 h at 60 °C only need about 1.5 and 6 h, proving a lurking application of ZJU-64 and ZJU-64-CH$_3$ as temperature sensitive drug nanocarriers.

Sometimes a single factor is not enough to stimulate the drug release efficiency of NMOFs due to the complexity of organism. Multiple stimuli-responsive MOFs can be served as a better choice to increase drug release efficiencies. Yang and co-workers constructed the first example of mono-disperse mechanized NMOFs by post modification mechanism using stimuli responsive molecules in which pillarene-based supramolecular switches act as gatekeepers (Tan et al., 2015). This nanocarrier has exhibited pH- and/or competitive binding-triggered responded drug release. Deeper research on NMOFs-based nanocarriers with multipoint stimulus response have also been did by the same group in which carboxylatopillar [5]arene (CP5) cyclic structure act as locker. Electrostatic interaction

TABLE 2 | The form of cancer treatment of various NMOFs as phototherapeutic agents for cancer therapy.

NMOFs	Photosensitizers (PSs)	Light source	Therapeutic agents	Form of cancer treatment	Refs
PB@MIL-100(Fe)	Prussian blue (PB)	NIR		PTT	Wang B et al. (2016)
PB@mSiO$_2$–PEG	Prussian blue (PB)	NIR	DOX	PTT	Su et al. (2016)
UiO-66@PAN	Polymer polyaniline (PAN)	NIR	-	PTT	Wang D et al. (2016)
PPy@MIL-100	Polypyrrole (PPy)	NIR	-	PTT and chemotherapy	Chen D et al. (2017)
MOF@HA@ICG	Indocyanine green (ICG)	NIR	-	PTT	Cai et al. (2017)
Hf$_6$(μ_3-O)$_4$ (μ_3-OH)$_4$ (DBP)$_6$	Porphyrin DBP	Visible light	$^1O_2$	PDT	Lu et al. (2014)
Hf$_6$(μ_3-O)$_4$ (μ_3-OH)$_4$ (DBP)$_6$	Porphyrin DBC	Visible light	$^1O_2$	PDT	Lu et al. (2015)
Hf-TCPP	Hf^{4+}, Porphyrin	X-ray	$^1O_2$	PDT and RT	Liu et al. (2016)
PCN-224	Zr^{4+}, Porphyrin	UV	$^1O_2$	PDT	Park et al. (2016a)
Zn-TCPP-BPDTE	Porphyrin TCPP	UV	$^1O_2$	PDT	Park et al. (2015)
UiO-66	TCPP	UV	$^1O_2$	PDT	Park et al. (2016b)
UiO-PDT	BODIPYs	Confocal laser	$^1O_2$	PDT	Wang et al. (2016a)
Hf-/Zr-based MOFs	[M$_6$]-clusters (M = Hf or Zr)	X-ray, visible light	photons	PDT	Wang et al. (2014)
Hf-BPY-Ir/Ru	Hf atoms	X-ray	$^1O_2$	PDT	Lan et al. (2017)
IDOi@TBC-Hf	Hf atoms	LED	$^1O_2$ and IDOi	PDT and immunotherapy	Lu Y et al. (2016)
DBP-Hf	Hf atoms	LED	$^1O_2$ and IDOi	PDT and immunotherapy	Lu et al. (2018a)
g-C$_3$N$_4$@ZIF-8	g-C$_3$N$_4$	-	$^1O_2$ and IDOi	PDT and immunotherapy	Chen et al. (2015)
PCN-222	Porphyrin	-	$^1O_2$ and DOX	PDT and immunotherapy	Liu et al. (2017)
MIL-88B	Porphyrin	-	MB and DOX	PDT and chemotherapy	Sharma et al. (2017)
F127-MnO$_2$-ZIF@DOX/C$_3$N$_4$	g-C$_3$N$_4$	NIR	$^1O_2$ and DOX	PDT and immunotherapy	Zhang Q et al. (2018)

between quaternary ammonium salt with positive charge that was coated on UiO-66-NH$_2$ and the negatively charged CP5 cycles could produce [2]pseudorotaxanes as multipoint stimulus response to control drug release.
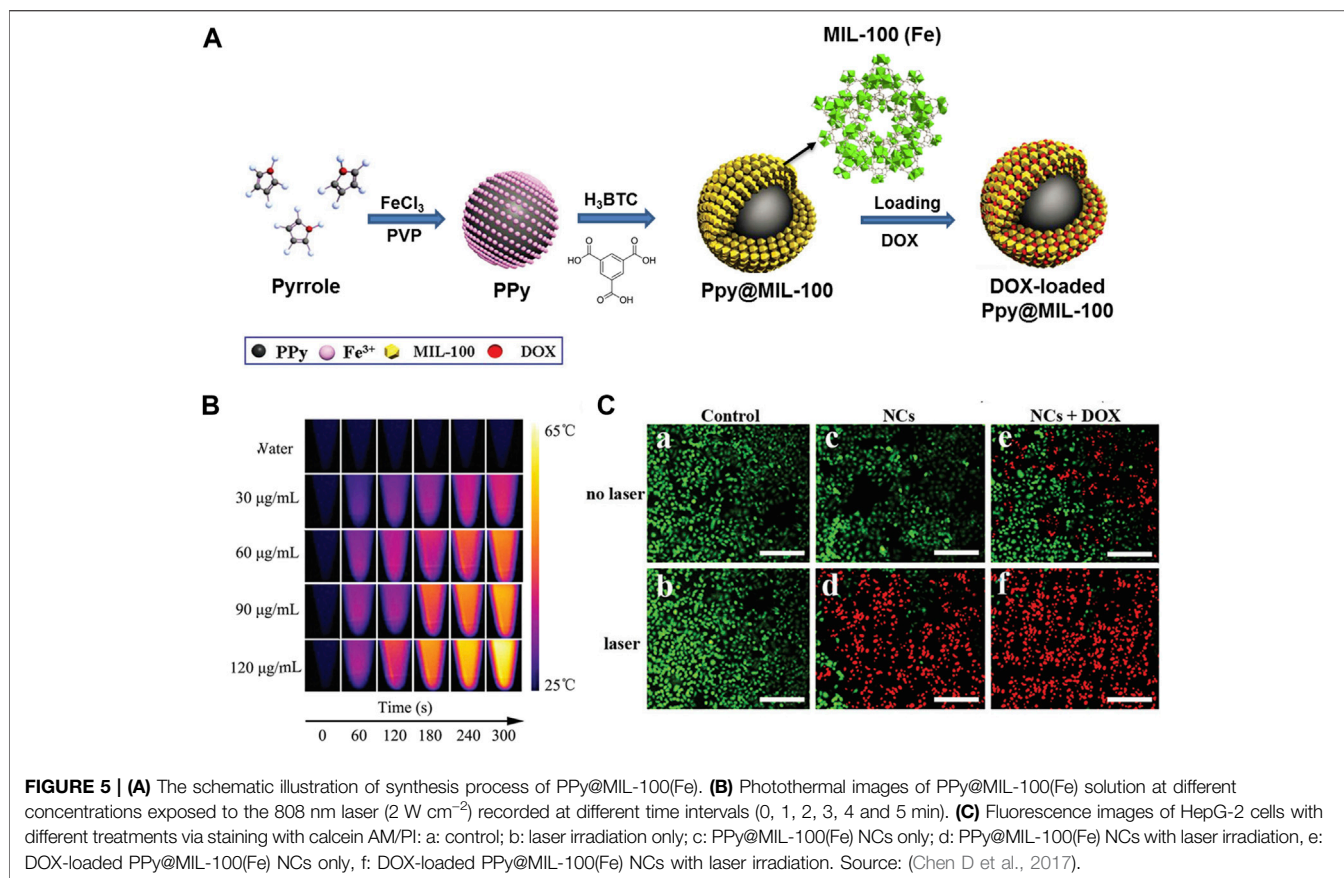
With the extensive research of NMOFs in the field of nanomedicine, some other factors that affect drug release also have been reported (Oh et al., 2015). Such as ion-responsive MOFs Zn$_8$ (ad)$_4$(BPDC)$_6$O·2Me$_2$NH$_2$·8DMF·11H$_2$O (bioMOF-1) (BPDC^{2-} = 4,4′-biphenyldicarboxylic acid) which was fabricated by Rosi group (An et al., 2009). Such anionic bio-MOF-1 could release a cationic drug (procainamide HCl) by the electrical reaction between cations and anions. Another case was given by Lin and co-workers, MIL-101 tethered drugs coated with silica shell could improve the drug release efficiency by prodrug hydrolysis because of the degradability of the silica shell in organism and phosphate buffered saline (PBS) solution (Taylor-Pashow et al., 2009). Moreover, pressure has been adopted for dominating drug release. Latterly, Qian groups designed a Zr-based MOF with high model drug diclofenac sodium (DS) loading amount up to 58.80 wt% (Jiang et al., 2016). The DS release kinetics could be controlled by regulating the pressure, resulting in a continual release between 2-8 days.

Nanoscale Metal–Organic Frameworks as Phototherapeutic Agents for Cancer Therapy

Cancer is one of the major diseases detrimental to health and is a major public health problem worldwide. With the enormous progress made in cancer biology in the past few decades, a large number of anticancer therapeutics have been brought to the clinic including small molecule inhibitors, antibodies, chemotherapeutics, and nucleic acid drugs. However, owing to

poor therapeutic effects, high risk of recurrence, intolerable side effects, and other reasons, conventional treatments often fail to meet clinical needs. Recently, phototherapeutic agents are widely used to treat cancer. However, due to the poor tissue penetration of light, pure phototherapy can only be used for superficial treatment. Adjustable structure, functional capabilities, biocompatibility, and biodegradability of NMOFs have made them a promising platform for cancer therapy. Noteworthy is the use of X-ray scintillating MOFs that constructed from metal cluster nodes of high atomic numbers (Z = 72 for Hf and Z = 40 for Zr). The Hf(IV) and Zr(IV) cations in the SBU act as antennas by absorbing X-ray photons and converting them to fast electrons through the photoelectric effect. The generated electrons scintillate/excite multiple anthracene-based optical emitters in the MOF through inelastic scattering, leading to efficient generation of detectable photons in the visible spectrum. Most importantly, NMOFs have the ability to preferentially deposit in tumors by enhancing permeability and retention (EPR) effect (Yang et al., 2020). In particular, the integration of photosensitizer to NMOFs not only addresses the limitations of photosensitizers, including aggregation, self-quenching, and uncontrollable *in vivo* but also improves loading efficiency, stability, and reduces cytotoxicity. **Table 2** summarizes the form of cancer treatment of various NMOFs as phototherapeutic agents for cancer therapy.

Photothermal therapy (PTT): PTT is a popular noninvasive method for converting the incident light energy into heat for degrading tumors or killing cancer cell effectively via a light absorbing agent (Ni et al., 2020b). For NMOFs, three methods can be adopted for assembly multifunctional NMOF-based therapy for enhanced PTT. First, enhanced photothermal conversion efficiency by functionalizing the SBUs and bridging linkers of NMOFs. Second, incorporate the functional moieties into the framework of NMOFs via post-synthetic modification or

FIGURE 5 | (A) The schematic illustration of synthesis process of PPy@MIL-100(Fe). **(B)** Photothermal images of PPy@MIL-100(Fe) solution at different concentrations exposed to the 808 nm laser (2 W cm^{-2}) recorded at different time intervals (0, 1, 2, 3, 4 and 5 min). **(C)** Fluorescence images of HepG-2 cells with different treatments via staining with calcein AM/PI: a: control; b: laser irradiation only; c: PPy@MIL-100(Fe) NCs only; d: PPy@MIL-100(Fe) NCs with laser irradiation, e: DOX-loaded PPy@MIL-100(Fe) NCs only, f: DOX-loaded PPy@MIL-100(Fe) NCs with laser irradiation. Source: (Chen D et al., 2017).
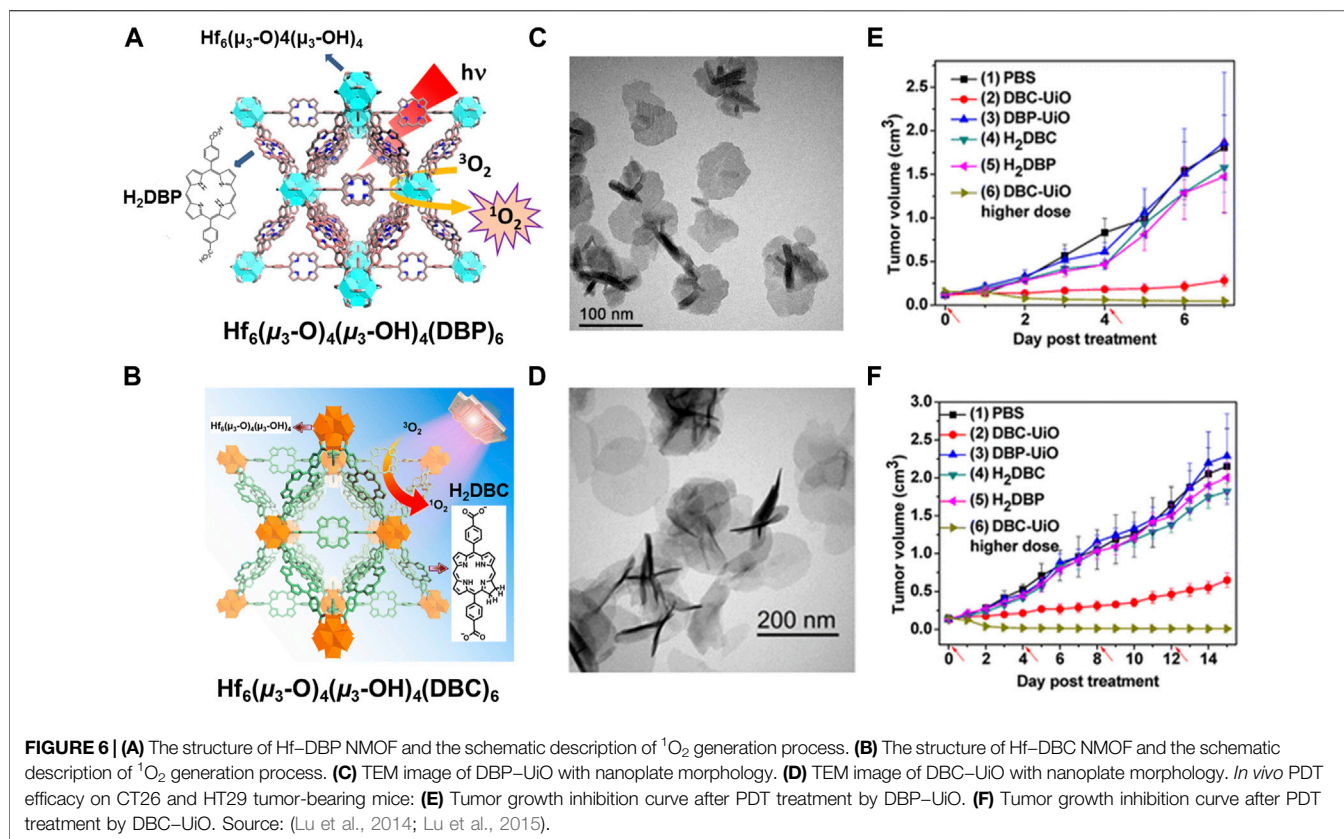
self-assembly from pre-modified linkers for the combination therapies. Third, by encapsulated the multifunctional agents into NMOF frameworks, the treatment efficiency of PTT could be improved. For example, Prussian blue (PB) is a prototype of mixed-valence hexacyanoferrate with a formula of $Fe_4^{III} [Fe^{II}(CN)_6]_3 \cdot nH_2O$ (Fu et al., 2012). Biosafety and wider absorption range of PB NPs make it outstanding phototherapeutic agents that can be embedded in the structure of MOFs to formed nanocomposites for PPT. Chen and coworkers obtained a multifunctional PB@MIL-100(Fe) dual-MOFs nanomaterial for combined chemotherapy and PTT and steps for the synthesis of dual-MOFs therapeutic nanoparticle (Wang B et al., 2016). Subsequently, Zhang and coworkers acquired PB@mSiO$_2$–PEG with a high antitumor drug DOX loading (Su et al., 2016). Under the irradiation of near-infrared laser, the constructed PB@mSiO$_2$–PEG/DOX nanoplatform exhibits efficacy photothermochemical therapy for breast cancer.

Besides PB, NIR-absorbing polymer polyaniline (PAN) also exhibit strong absorption coefficients and excellent photostability that could be incorporated in the channels of NMOFs to construct nanocomposites for PTT upon NIR laser irradiation. Jing and co-workers synthesized a nanoscale polymer-MOF hybrid named UiO-66@PAN, in which PAN had the NIR-absorbing ability (Wang D et al., 2016). The UiO-66@PAN is effective for PTT based cancer treatment both *in vivo* and *in vitro*.

As a result of higher photothermal transformation efficiency and outstanding biocompatibility, Polypyrrole (PPy) incorporated nanomaterial has been proved to be efficient for PTT. The fabrication process of PPy@MIL-100 was shown in **Figure 5A**, in which PPy and FeCl$_3$·6H$_2$O acted as a catalyst and PVP as stabilizer. The PPy core acts as a PTT agent while an organic PAI agent for deep tissue imaging. The MIL-100 shell was applied for loading DOX drugs. It was suggested that polypyrrole was formed by Fe(III) ions induced oxidative polymerization of PPy, then the combination of Fe(III) ions and polypyrrole surface promoted the formation of MIL-100 shell on PPy. Moreover, PPy@MIL-100 supported pH- and light controlled drug release, dual-modal imaging, and combined PTT and chemotherapy (**Figures 5B,C**). Besides this, Wang groups reported a dual-modal imaging core-shell nanomaterial PPy@MIL-100 for combined chemotherapy and PTT (Chen R et al., 2017). Indocyanine green (ICG) is the NIR optical dye and can be used for clinical applications. For example, Chen groups designed a multifunctional nanoplatform MOF@HA@ICG based on hyaluronic acid (HA) for imaging-guided PTT (Cai et al., 2017). Hovever, the lacked of sensitivity and specificity in cancer treatment limited its application.

Photodynamic therapy (PDT): Photodynamic therapy (PDT) is more effective anticancer treatment that depends on nontoxic photosensitizer (PS) to yield reactive oxygen species (ROS) to inhibit cancer cells (Horne and Cronjé, 2017). The first way of

FIGURE 6 | (A) The structure of Hf–DBP NMOF and the schematic description of $^1O_2$ generation process. **(B)** The structure of Hf–DBC NMOF and the schematic description of $^1O_2$ generation process. **(C)** TEM image of DBP–UiO with nanoplate morphology. **(D)** TEM image of DBC–UiO with nanoplate morphology. *In vivo* PDT efficacy on CT26 and HT29 tumor-bearing mice: **(E)** Tumor growth inhibition curve after PDT treatment by DBP–UiO. **(F)** Tumor growth inhibition curve after PDT treatment by DBC–UiO. Source: (Lu et al., 2014; Lu et al., 2015).

constructing NMOFs for PPT is using the nontoxic photosensitizer as building blocks. In 2014, Lin and co-workers first literates a Hf-porphyrin NMOFs with formula of $Hf_6(\mu_3\text{-O})_4 (\mu_3\text{-OH})_4 (DBP)_6$ (H_2DBP = 5,15-di (p-benzoato)-porphyrin) by a solvothermal strategy, as a significant photosensitizer for PDT (Lu et al., 2014). Thanks to position separation of porphyrin ligands, $Hf_6(\mu_3\text{-O})_4 (\mu_3\text{-OH})_4 (DBP)_6$ could efficiently generate $^1O_2$ to enhance intersystem crossing by heavy Hf centers, and realize $^1O_2$ invasive from the interior of MOFs to the cell through porous nanoplates, as shown in **Figures 6A,C**. Porous NMOF structure impelled $Hf_6(\mu_3\text{-O})_4 (\mu_3\text{-OH})_4 (DBP)_6$ remarkable PS loading up to 77 wt%. Moreover, in NMOF-treated group with 180 J cm^{-2} light dose, two quarters mouse had their tumors eradicated while the other two achieved 98% tumor regression, on contrary, the ligand control failed to inhibit the tumor growth at the same dose (**Figure 6E**). Then, the same group used another hematoporphyrin derivative 5,15-di (p-benzoato)-chlorin (H_2DBC) as ligand to coordinate with Hf and finally afforded a UiO framework of $Hf_6(\mu_3\text{-O})_4 (\mu_3\text{-OH})_4 (DBC)_6$ by solvothermal reaction (**Figure 6B**) (Lu et al., 2015). The $Hf_6(\mu_3\text{-O})_4 (\mu_3\text{-OH})_4 (DBC)_6$ NMOF is isostructural to $Hf_6(\mu_3\text{-O})_4 (\mu_3\text{-OH})_4 (DBP)_6$, showing a thin nanoplate morphology with thicknesses of 3.3–7.5 nm (**Figure 6D**). Importantly, compared to $Hf_6(\mu_3\text{-O})_4 (\mu_3\text{-OH})_4 (DBP)_6$, $Hf_6(\mu_3\text{-O})_4 (\mu_3\text{-OH})_4 (DBC)_6$ exhibits a 13 nm red shift and an 11-fold increase in the extinction coefficient of the lowest-energy Q-band that providing improved light penetration through tissues. Furthermore, $Hf_6(\mu_3\text{-O})_4 (\mu_3\text{-OH})_4 (DBC)_6$ is

3 times as efficient as $Hf_6(\mu_3\text{-O})_4 (\mu_3\text{-OH})_4 (DBP)_6$ in generating $^1O_2$ and exhibits much higher PDT cytotoxicity in two colon cancer cell lines (**Figure 6F**).

In addition to the above porphyrin derivatives, 5,10,15,20-tetrakis (4-carboxyphenyl) porphyrin (H_4TCPP) is a commercially available photosensitizer applied in PDT (Bůžek et al., 2017). The symmetrical molecular structure of TCPP and the strong coordination ability of its four carboxyl groups to metal ions could facilitate the formation of MOF structure. Liu groups obtained a NMOF Hf-TCPP composed by Hf^{4+} and TCPP and proved the ability for efficient PDT by intravenous injection (Liu et al., 2016). Hf-TCPP displayed spherical morphology structure and TCPP in Hf-TCPP act a photosensitizer to allow PDT. In addition, strong X-ray attenuation ability of Hf^{4+} could act as a radio-sensitizer to enhance radiotherapy (RT). Zhou group reported a series of Zr^{IV}-based porphyrinic NMOF (PCN-224) with different sizes (Park et al., 2015). The author indicated that modifing the surface of PCN-224 with folic acid could improve cell uptake of NMOFs and exhibited higher PDT efficacy.

Dithienylethene derivative, 1,2-bis(2-methyl-5-(pyridin-4-yl) thiophen-3-yl)cyclopent-1-ene (BPDTE) could serve as a photochromic switch to adopt reversible 6π electrocyclic reaction under photoirradiation at distinct wavelengths. The switch effect of BDPTE induced by light isomerization show special absorption characteristics, and can supply diverse energy transfer ways for photosensitizers to generate $^1O_2$. Meanwhile, dipyridyl head in BPDTE make it possible for forming pillar-layer
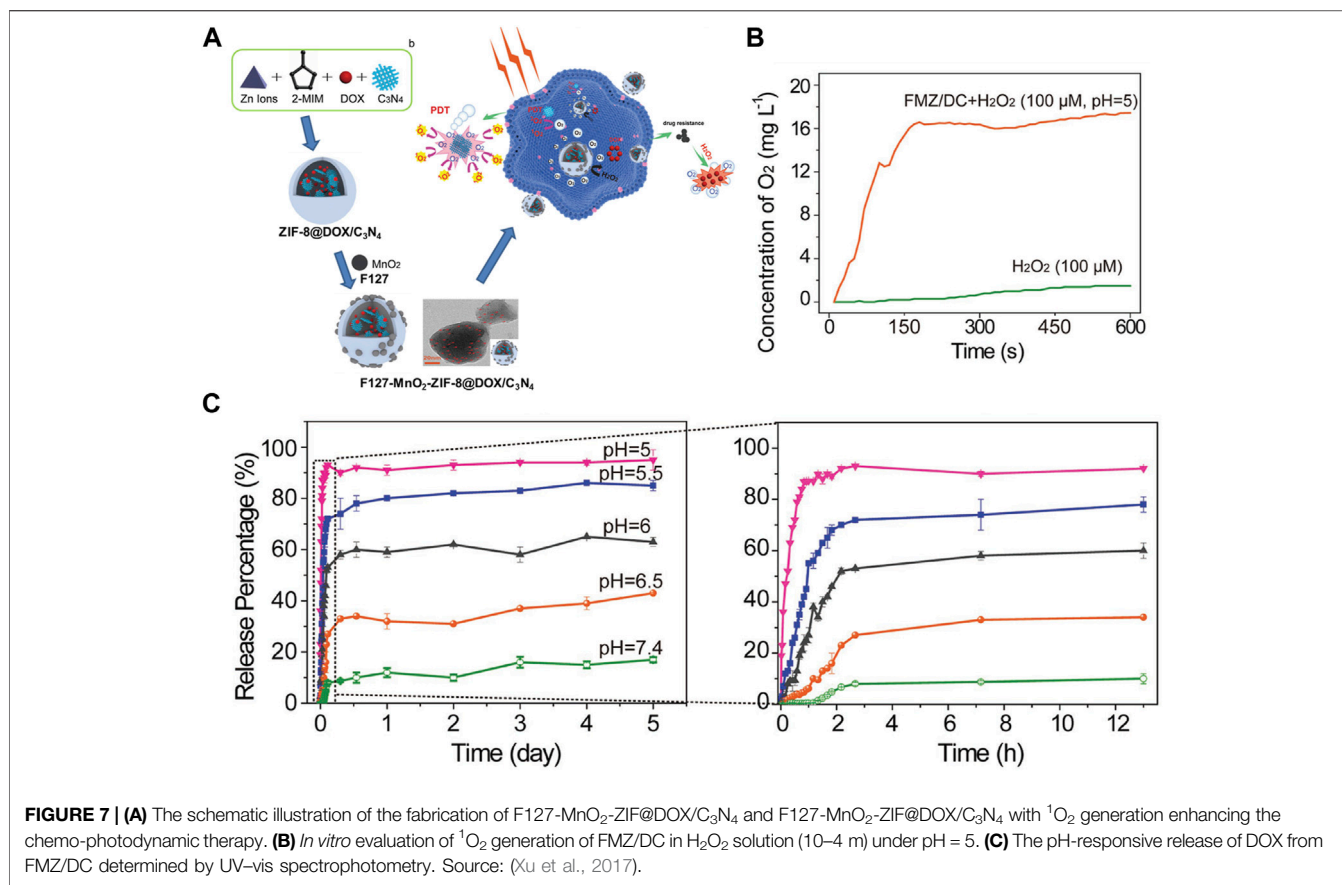
structure with TCPP to produce $^1O_2$. Zhou groups constructed Zn(II) based MOF (Zn-TCPP-BPDTE) by solvothermal reaction of TCPP (no metal), BPDTE, and $Zn(NO_3)_2 \cdot 6H_2O$. In Zn-TCPP-BPDTE, paddlewheel-type Zn cluster linked TCPP via Zn-O bonds and linked BPDTE through the Zn–N bonds (Park et al., 2015). Upon UV irradiation, Zn-TCPP-BPDTE could present switch effect owing to the photochromic property of BPDTE. Moreover, the "on" state of Zn-TCPP-BPDTE without impacting the $^1O_2$ generation of TCPP, but the BPDTE in "off" state of Zn-TCPP-BPDTE extinguished the S_1 state of TCPP to decrease $^1O_2$ generation. Later, they used the same technique obtained a UiO-66 NMOF-based $^1O_2$ generation platform in which 1,2 bis(5-(4-carbonxyphenyl)-2-methylthien-3-yl) cyclopent-1-ene (BCDTE) as the photochromic switch and TCPP ligand as the PS (Park et al., 2016a). The cytotoxicity test showed that PDT cytotoxicity in the "on" state of BCDTE doped UiO-66 is ~90%, while in the "off" state only 10%. This result proved the method of encapsulating photochromic molecules and PSs together into NMOFs to regulate $^1O_2$ generation efficacy and finally impact in vitro PDT.

Ligand exchange offers another way for fabricating NMOFs for PDT. Xie and co-workers incorporated the carboxyl-modified diiodo-substituted BODIPYs (I2-BDP) into UiO-66 to elaborate the PDT into the product of UiO-PDT through solvent-assisted ligand exchange (Wang et al., 2016a). Structural analysis shows that there was 12.5 mol% of benzenedicarboxylate linker was exchanged by carboxy-I2-BDP in UiO-PDT and affording a PS loading of 31.4 wt%. Both UiO-PDT and carboxy-I2-BDP had the ability of crossing the cell membrane to accumulate in the cytoplasm through Confocal laser scanning microscopy study. The penetration of light affects efficiency of NMOFs for PDT as well as the building blocks in anticancer treatment. Compared with visible light and near-infrared, X-rays have stronger penetrability in organism and have been widely employed in cancer treatment (Song et al., 2018). Lin and co-workers did outstanding work on efficiently converting X-ray to visible-light luminescence of NMOFs for PDT. In 2014, they first designed and synthesized X-ray Hf-/Zr-based MOFs with formula of M_6 $(\mu_3\text{-}O)_4$ $(\mu_3\text{-}OH)_4$ (carboxylate)$_{12}$ (M = Hf or Zr) (Wang et al., 2014). The high atomic number of $[M_6]$-clusters in the SBUs acts as effective X-ray antenna by absorbing X-ray photons and transforming them into fast electrons. Once the $[M_6]$-clusters assimilated X-rays in the energy range of 20–200 keV, the outer electrons of M^{4+} were emitted in the form of fast electrons to produce visible light. The X-ray-induced emission spectra exhibited that the emission peaks of M_6 $(\mu_3\text{-}O)_4$ $(\mu_3\text{-}OH)_4$ (carboxylate)$_{12}$ was in the visible range of 400–600 nm. Obviously, this visible light had potential for serve as a PDT light source. In 2017, they built two Hf-based nanomaterials Hf-BPY-Ir or Hf-BPY-Ru as powerful PSs for effective X-PDT of colon cancer models in which $[Hf_6O_4(OH)_4(HCO_2)_6]$ as SBUs and Ir [bpy (ppy)$_2$]$^+$- or [Ru (bpy)$_3$]$^{2+}$- as ligands (bpy = 2,2'-bipyridine, ppy = 2-phenylpyridine) (Lan et al., 2017). Hf-BPY-Ir was obtained by reacting [Ir (ppy)$_2$Cl]$_2$ and Hf-based MOF in a post-synthesis modification strategy (H$_3$BPY = 4',6'-dibenzoato-[2,2'-bipyridine]-4-carboxylic acid). Similarly, Hf-BPY-Ru

nanomaterial were designed using Ru (bpy)$_2$Cl$_2$. Heavy Hf atoms in the SBUs absorb X-rays efficiently and transfer the energy to Ir [bpy (ppy)$_2$]$^+$ or [Ru (bpy)$_3$]$^{2+}$ units to lead to PDT by generating ROS. The fabricated cell experiment showed that these two nanomaterials had an excellent inhibitory effect on CT26 and MC38 cells in vitro, while in vivo experiments proved the efficient penetration of X-rays into tumor to enable efficient deep PDT which was performed in amice.

Combined theranostic strategies: Although PTT and PDT can strengthen by diverse strategies; the effect of monotherapy is still not satisfactory. Up to now, cancer treatment has gradually shifted from monotherapy to combination therapy which means integrating of two or more treatments for synergistic effects (Zhang et al., 2020). In 2016, Lin and co-workers obtained IDOi@TBC-Hf nanomaterial with chlorin derivative, 5,10,15,20-tetra (pbenzoato) chlorin (H$_4$TBC) and Hf$_6$(μ_3-O)$_4$ (μ_3-OH)$_4$ in which IDOi was loaded (Lu Y et al., 2016). Through the combination of NMOF-enabled PDT and IDOi-based immunotherapy, IDOi@TBC-Hf platform makes a possible cancer therapy strategy. Mechanistic studies suggested that ROS were generated upon irradiation after the local injection of IDOi@TBC-Hf leading immunogenic cell death and the release of tumor associated antigen. Subsequently, the same group obtained a series of IDOi-loaded NMOFs as a treatment therapy that synergized checkpoint blockade immunotherapy and low doses of X-ray-excited PDT to acquire effective local control and abscopal effects in mice models, including DBP-Hf (H$_2$DBP = 5,15-di (p-benzoato)porphyrin), TBP-Hf (H$_4$TBP = 5,10,15,20-tetra (p-benzoato) porphyrin), DBA-Hf$_6$ and DBA-Hf$_{12}$ (H$_2$DBA = 2,5-di (p-benzoato)aniline) (Lu et al., 2018b). The combination of X-ray-induced PDT and immunotherapy can not only reduce the possible various effects of local X-ray radiation but also eradicate both treated primary tumors and untreated distant tumors efficiently via systemic antitumor immune responses.

The major defects of chemotherapy are intolerable side effects, systemic toxicity, and multidrug resistance. When united the PDT and chemotherapy, PDT-induced photochemical internalization can significantly improve the efficacy of chemotherapy (Ni et al., 2018). Such as the encapsulation of anticancer drug DOX into the NMOF with photodynamic effect not only could meet high loading rate of DOX but also could facilitate the induction of $^1O_2$ production because of the high content of PS in the NMOFs. Lee and co-workers produced a core-shell structure g-C$_3$N$_4$@ZIF-8 for DOX drug delivery (Chen et al., 2015). The anticancer efficacy of g-C$_3$N$_4$@ZIF-8 enhanced significantly by combination DOX with g-C$_3$N$_4$. Besides ZIF-8, PCN-222 was also used as a nanocarrier for loading DOX and PDT (Liu et al., 2017). 109 wt% loading rate of DOX was obtained due to the larger pore channel (1.75V 1.75 nm). In addition, $^1O_2$ production could be facilitated by the high concentrations of porphyrin (59.8 wt%) in the PCN-222. Similarly, Roy and co-workers acquired a combination of PDT and chemotherapy by incorporated MB and DOX into the micropores of MIL-88B (Sharma et al., 2017). In order to effectively strengthen the antitumor effect, Wang and co-workers obtained F127-MnO$_2$-ZIF@DOX/C$_3$N$_4$ nanomaterial with integration of chemotherapy

FIGURE 7 | (A) The schematic illustration of the fabrication of F127-MnO$_2$-ZIF@DOX/C$_3$N$_4$ and F127-MnO$_2$-ZIF@DOX/C$_3$N$_4$ with ^{1}O$_2$ generation enhancing the chemo-photodynamic therapy. **(B)** *In vitro* evaluation of ^{1}O$_2$ generation of FMZ/DC in H$_2$O$_2$ solution (10–4 m) under pH = 5. **(C)** The pH-responsive release of DOX from FMZ/DC determined by UV–vis spectrophotometry. Source: (Xu et al., 2017).

and aerobic PDT, which had a fairly good curative effect on hypoxic tumors (Zhang Q et al., 2018). Particularly, the g-C3N4 PS and the DOX drugs were incorporated into the ZIF-8 by electrostatic interactions finally obtained F127-MnO$_2$-ZIF@ DOX/C$_3$N$_4$ nanomaterial (**Figure 7A**). F127 improved the biocompatibility the nanomaterial, promoting its accumulation in cancer (**Figure 7B**). ZIF-8 offered pH-responsive characteristics for the nanomaterial: releasing DOX under acidic conditions, reducing side effects, and reducing nonspecific drug release (**Figure 7C**). In addition, the loaded MnO$_2$ nanodots could continuously catalyze the decomposition of endogenous H$_2$O$_2$ to produce O$_2$, and greatly enhance the PDT effect.

Nanoscale Metal–Organic Frameworks as Fluorescent Probe for Biomedical Sensing and Imaging

Biomedical sensing and imaging have been proved as prospecting pattern for detection multiple complexes selectively and rapidly as well as environmental safety (Dong et al., 2019). Luminescent characteristics together with size/shape selective sorption properties of NMOFs make them potential fluorescent probe for biomedical sensing and imaging under different mechanisms. So far, various NMOFs were explored for detecting DNA/RNA, enzyme activity and small-biomolecules, as well as magnetic

resonance imaging (MRI), X-Ray computed tomography (CT), positron emission tomography (PET) and optical imaging, which are useful techniques for clinical diagnosis.

Biomedical sensing: Through overcoming the self-quenching and leaching problems of many small molecular biosensors, NMOF-based sensors realize high sensitivity, high precision, and high resolution in subcellular bioprobes. Recently, a lot of studies have reported to describe the NMOFs as sensitive and selective sensors for screening biological macromolecules like nucleic acids (Yang Y et al., 2017), and proteins (Xu et al., 2017), small biomolecules including glucose (Chen et al., 2016), amino acids (Wang et al., 2015), and so on in cellular and subcellular sensing, as shown in **Table 3**.

The most exciting stories of the biomolecular sensing applications of NMOFs have been found from screening nucleic acid molecules, such as DNAs and RNAs. The detecting of DNAs and RNAs by NMOFs were mainly realized by anchoring NMOFs to nucleic acid molecules detectors. For instance, in order to detect the human immunodeficiency virus (HIV-1), a N,N'-bis(2-hydroxyethyl) dithiooxamidato containing NMOF named [Cu(H$_2$dtoa)] has been synthetized (Zhu et al., 2013). The sensing mechanism of this detecting platform is to regenerate the photoluminescence intensity of the carboxyfluorescein (FAM)-labeled probe DNA by binding specific DNA with MOFs. With the similar quenching principle, NMOF with formula of [Cu$_3$(Cmdcp)$_2$
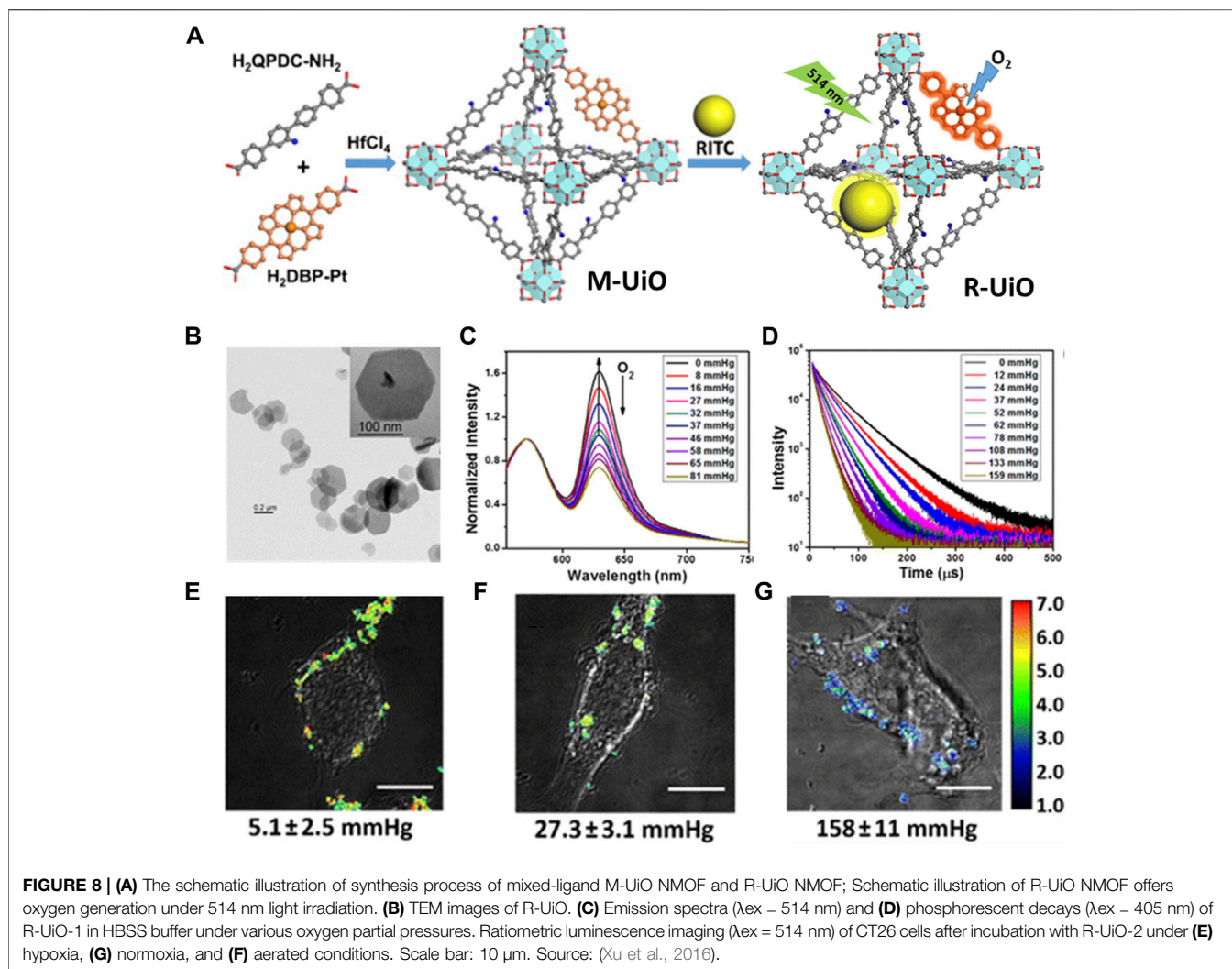
TABLE 3 | Various NMOFs as sensitive and selective sensors for screening biological macromolecules.

NMOFs	Probe units	Biomolecules	Detection limit	Detection mechanism	Refs
[Cu(H$_2$dtoa)]	FAM-labeled probe	HIV-1 (DNA), Thrombin	-	PET	Zhu et al. (2013)
[Cu$_3$(Cmdcp)$_2$ (dps)$_4$·(H$_2$O)$_4$(SO$_4$)]$_n$	FAM-labeled probe	HIV-1 (dsDNA) and Sudan virus RNA	196 pM for DNA, 73 pM for RNA	PET	Yang et al. (2015)
{[Dy(Cmdcp)(H$_2$O)$_3$](NO$_3$· 2H$_2$O}$_n$	-	Ebolavirus RNA	160 pM for RNA	π-stacking and/or hydrogen bonding	Qin et al. (2016)
{[La$_4$(Cmdcp)$_6$(H$_2$O)$_9$]}$_n$	FAM-labeled probe	P-DNA	-	PET	
{[La$_2$(Cbdcp)$_3$(H$_2$O)$_{10}$]}$_n$	FAM-labeled probe	DNA or RNA	-	PET	Yang S P et al., 2017, Zhao et al. (2016a), Zhao et al. (2016b)
{[Zn(HCbdcp)$_2$]H$_2$O}$_n$ [Cu(dcbb)$_2$]$_n$ {[Cu(dcbb)$_2$(H$_2$O)$_2$]· 10H$_2$O}$_n$					
UiO-66-NH$_2$	FAM-labeled probe	HIV-1 (DNA)	-	Electrostatic and π-π stacking	Fang et al. (2014), Mejia-Ariza et al. (2017), Zhao H X et al. (2016), Ling et al. (2015)
UiO-66 MIL-101 MIL-88A [Gd (TIA)(HCOO)]$_n$ {[La$_2$ (TDA)$_3$]·2H$_2$O}$_n$ Cd(L)·(HDMA)$_2$ (DMF)(H$_2$O)$_3$ Zn(L)·(HDMA)$_2$ (DMF)(H$_2$O)$_6$					
[Cd (ATC)(H$_2$O)$_2$]$_n$	Functional (-COOH/-NH$_2$) groups	anti-BSA	7 mg/ml	-	Kumar et al. (2014)
[Cu(mal)(bpy)]·2H$_2$O	FAM-labeled probe	glycine (Gly) and serine (Ser)	0.81 μg ml^{-1} for Gly, 1.51 μg ml^{-1} for Ser	-	Li S Y et al. (2017)
{[Cd(L)(bpy)]·DMA·5H$_2$O}$_n$	π-conjugated naphthyl moiety	penicillamine (PEN)	23.72 μM^{-1} for D-PEN, 10.13 μM^{-1} for L-PEN	-	Zhang W et al. (2018)
R-UiO	Oxygen-responsive phosphorescent ligand	ROS	-	-	Xu et al. (2016)
Zr$_6$O$_4$(OH)$_8$(H$_2$O)$_4$(CTTA)$_{8/3}$	-	NZF and TNP Antibiotics	58 ppb NZF, 23 ppb TNP	Electron transfer and energy transfer	Wang et al. (2016b)
Zr$_6$O$_4$(OH)$_8$(H$_2$O)$_4$ (TTNA)$_{8/3}$			58 ppb NZF, 23 ppb TNP		
[Cd$_2$Na(L)(BDC)$_{2.5}$]·9H$_2$O	-	NZF antibiotics	162 ppb	Electron transfer and energy transfer	Zhao et al. (2017)
[Cd$_2$(L)(2,6-NDC)$_2$]· DMF·5H$_2$O			75 ppb		
[Cd$_2$(L)(BPDC)$_2$]·DMF·9H$_2$O			60 ppb		

(dps)$_4$·(H$_2$O)$_4$(SO$_4$)]$_n$ (H$_3$CmdcpBr = N-carboxymethyl-3,5-dicarboxylpyridinium bromide; dps = 4,4′-dipyridyl sulphide) was also used for detecting of HIV-1 double-stranded DNA (dsDNA) and Sudan virus RNA (Yang et al., 2015). Later, the research group used lanthanides ions and the identical inorganic linker to obtained {[La$_4$(Cmdcp)$_6$(H$_2$O)$_9$]}$_n$ and {[Dy(Cmdcp)(H$_2$O)$_3$](NO$_3$·2H$_2$O}$_n$ with water stability (Qin et al., 2016). The coordinated water molecules and free NO$_3^-$ anions on the channels of {[Dy(Cmdcp)(H$_2$O)$_3$](NO$_3$·2H$_2$O}$_n$ can induce electrostatic and hydrogen bonding interactions with FAM-tagged probe DNA. Moreover, the transient complex formed by NMOFs and FAM-tagged probe DNA served as high efficiency and selectivity fluorescent probes for sensing Ebolavirus RNA. MOF {[La$_4$(Cmdcp)$_6$(H$_2$O)$_9$]}$_n$ can absorb FAM-tagged probe DNA and quench the fluorescence of FAM through a photo-induced electron transfer (PET) process. Similarly, other water-stable NMOFs {[La$_2$(Cbdcp)$_3$(H$_2$O)$_{10}$]}$_n$ (H$_3$CbdcpBr = N-(4-carboxybenzyl)-3,5-dicarboxylpyridinium

bromide), {[Zn(HCbdcp)$_2$]H$_2$O}$_n$, [Cu(dcbb)$_2$]$_n$ (H$_2$dcbbBr = 1-(3,5-dicarboxybenzyl)-4,4′-bipyridinium bromide) and {[Cu(dcbb)$_2$(H$_2$O)$_2$]·10H$_2$O}$_n$ also have been reported for sensing virus DNA or RNA by absorbing FAM-tagged probe DNA and inhibited the fluorescence of FAM by PET (Zhao et al., 2016a; Zhao et al., 2016b; Yang S P et al., 2017).

Additionally, UiO-66-NH$_2$, UiO-66, MIL-101, MIL-88A, {[La$_2$ (TDA)$_3$]·2H$_2$O}$_n$ (TDA = 2,2′-thiodiacetic acid), [Gd (TIA)(HCOO)]$_n$ (TIA = 5-triazole isopthalate), Cd(L)·(HDMA)$_2$ (DMF)(H$_2$O)$_3$ and Zn(L)·(HDMA)$_2$ (DMF)(H$_2$O)$_6$ (H$_4$L = bis-(3,5-dicarboxy- phenyl) terephthalamide, DMA = N,N-dimethylacetamide) (Fang et al., 2014; Ling et al., 2015; Zhao H X et al., 2016; Mejia-Ariza et al., 2017) have also been used as fluorescent probes for DNA/RNA and is able to distinguish complementary and mismatched target sequences with good selectivity and sensitivity. Besides biological molecular DNA/RNA, proteins can also be identified by NMOFs. MOF [Cd (ATC)(H$_2$O)$_2$]$_n$ (ATC = 2-aminoterephthalic acid) has

FIGURE 8 | (A) The schematic illustration of synthesis process of mixed-ligand M-UiO NMOF and R-UiO NMOF; Schematic illustration of R-UiO NMOF offers oxygen generation under 514 nm light irradiation. **(B)** TEM images of R-UiO. **(C)** Emission spectra (λex = 514 nm) and **(D)** phosphorescent decays (λex = 405 nm) of R-UiO-1 in HBSS buffer under various oxygen partial pressures. Ratiometric luminescence imaging (λex = 514 nm) of CT26 cells after incubation with R-UiO-2 under **(E)** hypoxia, **(G)** normoxia, and **(F)** aerated conditions. Scale bar: 10 μm. Source: (Xu et al., 2016).

recently been proposed as a molecular sensing platform for the fluorescence quenching based detection of bovine serum albumin (anti-BSA) through activate -COOH/-NH$_2$ groups followed by the attachment of proteins (Kumar et al., 2014). Limit of detection or the proposed detection is found to be 7 mg/ml that is comparable to the quantum dot based detections.

Besides the DNA/RNA and proteins biological macromolecular, NMOFs can also serve as fluorescence sensors to distinguish amino acids (Wang and Wei, 2016). Pioneering work on amino acids recognition includes the detection of dipicolinic acid (DPA) molecules, a structural constituent of *bacillus* anthrasis spores and many other virulent bacteria. Particularly, MOF named [Cu(mal)(bpy)]· 2H$_2$O (mal = D, L-malic acid) was constructed by Kong groups, a fluorescence probe experiment indicated that this MOF could act as fluorescence sensor to recognize glycine (Gly) and serine (Ser) and with low detection limits 0.81 μg ml^{-1} for Gly and 1.51 μg ml^{-1} for Ser (Li Y et al., 2017). The sensing principle is that fluorophore-labeled ssDNA can be adsorbed in [Cu(mal)(bpy)]·2H$_2$O, and then quenching of the fluorescence. In term of chiral precursors 4,4'-((naphthalene-1,4-

dicarbonyl)bis (azanediyl))dibenzoic acid (H$_2$L) and bpy, a 3D homochiral LMOF {[Cd(L)(bpy)]·DMA·5H$_2$O}$_n$ was successfully obtained by Zhang and co-works and can be used as detecting platform for distinguishing D/L-penicillamine (PEN) by the π-conjugated naphthyl groups as fluorescent emission center (Zhang W et al., 2018). Once excited {[Cd(L)(bpy)]· DMA·5H$_2$O}$_n$ under 340 nm, a quite strong fluorescence was obtained. By adding the D-PEN or L-PEN into this platform, the luminescence intensity quenched obviously. The linear range of this fluorescence sensor is from 20 to 167 μM, and the detection limits of D-Pen and L-Pen are 23.72 μM^{-1} and 10.13 μM^{-1}, respectively.

A variety of diseases cause hypoxia. PDT, radiation therapy and other common cancer treatment are all heavily oxygen-dependent treatments, so intracellular ROS sensing is greatly important and necessary. A phosphorescence/fluorescence dual-emissive NMOF was designed by Lin groups, namely, R-UiO, which could be used as an intracellular ROS detector (Xu et al., 2016). The R-UiO was stable, porous, crystalline, and dual emissive (**Figures 8A,B**). The mix-ligand R-UiO including an oxygen-responsive phosphorescent ligand, Pt-5,15-di

TABLE 4 | Various NMOFs as contrast agents for biomedical imaging.

NMOFs	Active ingredient	Contrast media	Biomedical imaging technologies	Refs
$Gd(BDC)_{1.5}(H_2O)_2$	Ga^{3+} ion	T1-weighted MRI	MRI	Rieter et al. (2006)
Gd-Ru	Ga^{3+} ion	T1-weighted MRI	MRI	Wang Y M et al. (2016)
Mn-NMOF	Mn^{2+} ion	T1-weighted MRI	MRI	Yang et al. (2016)
MIL-88A	Fe^{3+} ion	T2-weighted MRI	MRI	Horcajada et al. (2010)
MIL-100	Fe^{3+} ion			
Fe_3O_4@UiO-66	Fe_3O_4 nanoparticle	T2-weighted MRI	MRI	Zhao S N et al. (2016)
Zr-UiO	Zr^{3+} ion	-	CT	Kalra et al. (2004)
Hf-UiO	Hf^{4+} ion			
Au@MIL-88(Fe)	Fe^{3+} ion	T2-weighted MRI	MRI and CT	Shang et al. (2017)
Mn/Hf-IR825	Mn^{2+} ion	-	MRI and CT	Yang Y et al. (2017)
^{89}Zr-UiO-66	Zr^{3+} ion	-	PET	Chen D et al. (2017)
UCNP@Fe-MIL-101-NH$_2$	Fe^{3+} ion	T2-weighted MRI	Optical imaging and MRI	Li et al. (2015)
MOF@HA@ICG	indocyanine green (ICG) NIR dye Fe^{3+} ion	-	Optical imaging and PPT	Cai et al. (2017)

(p-benzoato)porphyrin, as an O^{2-} sensitive probe. Then, by thiourea bonds, the RhB was covalently bonding to the amino agents in amino-quaterphenyldicarboxylate as an oxygen-independent reference. The phosphorescence/fluorescence emissions were totally independent of each other by agents sharing the same excitation energy (**Figures 8C,D**). The determination of oxygen content in hypoxia, normoxia, and aerated cells was realized by live-cell confocal microscopic imaging (**Figures 8E–G**).
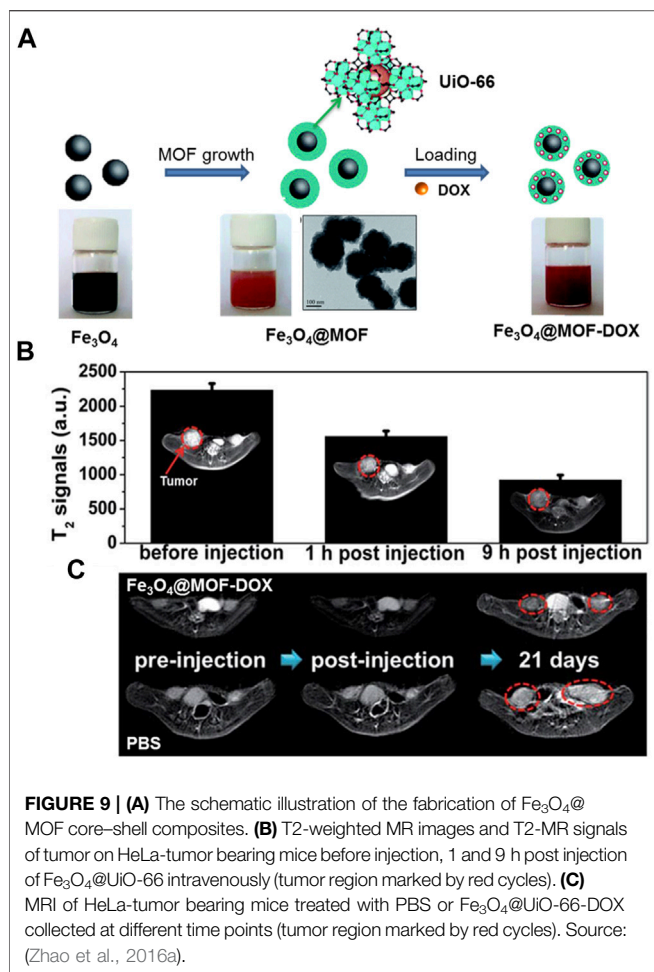
Antibiotics are mainly used for infections caused by bacteria. Antibiotic resistance not only has a serious impact on human and animal health, but also can be widely spread as antibiotic wastes (Zhu et al., 2018). Due to the rapid response, highly selectivity and sensibility, the biosensors based on fluorescent MOF for antibiotic detection became popular. By adopting high-Z ions Zr^{4+} and fluorescent inorganic linkers H$_3$CTTA (5'-(4-carboxyphenyl)-2',4',6'-trimethyl-[1,1':3',1''-terphenyl]-4,4''-dicarboxylic acid)) and H$_3$TTNA (6,6',6''-(2,4,6-trimethylbenzene-1,3,5-triyl)tris (2-naphthoic acid)), two Zr-MOFs Zr$_6$O$_4$(OH)$_8$(H$_2$O)$_4$(CTTA)$_{8/3}$ and Zr$_6$O$_4$(OH)$_8$(H$_2$O)$_4$ (TTNA)$_{8/3}$ were constructed by Zhou's group for sensing antibiotics effectively (Wang et al., 2016b). It was indicated that the excellent adsorption ability of these two complexes could remarkable increase the quenching efficiency and detection sensitivity for detecting and removing nitrofurazone (NZF) and nitrofurantoin (NFT) antibiotics. Recently, the author of this review designed a class of Cd(II)-based LMOFs named [Cd$_2$Na(L)(BDC)$_{2.5}$]·9H$_2$O, [Cd$_2$(L)(2,6-NDC)$_2$]·DMF·5H$_2$O and [Cd$_2$(L)(BPDC)$_2$]·DMF·9H$_2$O (1,4-NDC^{2-} = 1,4-naphthalenedicarboxylate) by introducing chelated polyamine linker N^1-(4-(1H-1,2,4-triazole-1-yl)benzyl)-N^1-(2-aminoethyl) ethane-1,2-diamine (L). The detecting experiments indicated that these Cd-MOFs can act as potential luminescence probes for detecting antibiotics. The fluorescence intensity of these materials can be inhibited efficiently by trace amount of NZF with detection limits are about 162, 75 and 60 ppb, respectively (Zhao et al., 2017).

Biomedical imaging: The advent of biomedical imaging technologies has extremely facilitated the diagnosis of devious diseases. Imaging methods could use either fluorescence and magnetism property, that the later one is more frequent reported in reports particularly in the applications involving NMOFs in which non-ionizing non-radioactive radiation could be used to generate images. By merits of their metal connecting points or nodes, NMOFs have been proved to be outstanding contrast agents for magnetic resonance imaging (MRI), optical imaging, X-ray computed tomography (CT), and PET (Khooa et al., 1997), as shown in **Table 4**.

Magnetic Resonance Imaging (MRI). As a powerful noninvasive imaging technique, MRI contrast agents facilitate optimal tumour evaluation by positive and negative contrast media to shorten the longitudinal (T1) relaxation rates and/or reduce the transverse (T2) relaxation rates of water protons to enhance MRI.

Currently, transitional metal ion (Gd^{3+} or Mn^{2+}) are generally used to construct T1 contrast agents for MRI by chelated structure to decrease severe side effects. The first example of Gd^{3+}-containing NMOFs as MRI contrast agents was constructed by Lin groups, namely $Gd(BDC)_{1.5}(H_2O)_2$ (Rieter et al., 2006). $Gd(BDC)_{1.5}(H_2O)_2$ nanopartical shows an r_1 relaxivity of 35.8 s^{-1} per mm Gd^{3+} or $\approx 1.6 \times 107$ mm^{-1} s^{-1} on a per NMOF basis. The r_1 relaxivity level of $Gd(BDC)_{1.5}(H_2O)_2$ is approximately an order of magnitude higher than the usually used technology Omniscan. Recently, by a hydrothermal treatment of Gd^{3+} and Ru(II)[4,4'-(COOH)$_2$ bipyridyl (bpy)]$_3$·Cl$_2$ (L$_{Ru}$), Yin groups acquired a kind of nanomaterial based on Gd^{3+} and L$_{Ru}$ precursors and used for MRI, namely Gd-Ru (Wang Y M et al., 2016). SEM and TEM images indicated that Gd-Ru is in globular structures of regular shape and uniform size in a mean diameter of 138 nm. Higher MRI contrast efficiency was acquired by Gd-Ru in contrast to the commercial MRI contrast Gd–DTPA (DTPA, diethylenetriamine pentaacetic acid). Although Gd^{3+} based nanomaterial have shown good MRI ability, but the possible release of toxic Gd^{3+} ions from Gd^{3+}-based nanoparticles hinders their deeper exploration for MRI. To settle the problem of toxicity of Gd-based NMOFs, Mn^{2+}-based NMOFs have been extensively investigated. As an example, Lin and coworkers designed Mn-BDC and Mn-BTC NMOFs for an optional MRI contrast media by reverse-phase microemulsion techniques at room temperature and a surfactant-assisted procedure at 120°C with microwave heating (Yang et al.,

FIGURE 9 | (A) The schematic illustration of the fabrication of $Fe_3O_4@$ MOF core–shell composites. **(B)** T2-weighted MR images and T2-MR signals of tumor on HeLa-tumor bearing mice before injection, 1 and 9 h post injection of $Fe_3O_4@UiO-66$ intravenously (tumor region marked by red cycles). **(C)** MRI of HeLa-tumor bearing mice treated with PBS or $Fe_3O_4@UiO-66$-DOX collected at different time points (tumor region marked by red cycles). Source: (Zhao et al., 2016a).

2016). The r_1 and r_2 relaxivities of Mn-BDC NMOF were 5.5 and 80.0 mm^{-1} s^{-1} on a per Mn basis, respectively.

The T2-weighted MRI contrast media is generally superparamagnetic iron oxides (SPIOs) which cause negative image enhancement. Not long ago, a series of ironcarboxylate NMOFs were synthesized by Horcajada and co-workers as T2-weighted contrast media (Horcajada et al., 2010). The size of these NMOFs range from 50 to 350 nm, matching known bulk phase materials of MIL-53, MIL-88A, MIL-88Bt, MIL-89, MIL-100, MIL-101-NH$_2$, PEG-MIL-88A and PEG-MIL-100 exhibited high r_2 relaxivity on a per metal basis and negative enhancement of the liver and spleen was observed after injection of MIL-88A, By incorporating Fe_3O_4 nanoparticles into the UiO-66, Fu groups acquired a core–shell nanomaterial $Fe_3O_4@UiO-66$ (Zhao S N et al., 2016), as shown in **Figure 9A**. Drug DOX was used to assessment the drug loading ability of the $Fe_3O_4@$ UiO-66 and incorporated into the framework of $Fe_3O_4@UiO-$ 66 to obtain $Fe_3O_4@UiO-66$-DOX. The generated $Fe_3O_4@$ UiO-66-DOX can not only act as nanoplatform for simultaneous drug delivery, but also can serve as a contrast media for T2-weighted MRI (**Figure 9B**). Moreover, $Fe_3O_4@UiO-66$-DOX could effectively inhibit

the growth of tumor, and the MRI of HeLa-tumor bearing mice injected with $Fe_3O_4@UiO-66$-DOX revealed obvious darkening effect in the tumor area (**Figure 9C**).

X-Ray Computed Tomography Imaging (CT). CT imaging is a noninvasive clinical diagnosis technique for 3D visualization of internal structures of a scanned object by X-ray attenuation. Contrast agents with high-Z ions, such as small molecular contrast media including iodinated aromatic molecules and barium sulfate, normally exhibit strong X-ray attenuation (Kalra et al., 2004). For the high-Z elements can be facile merged into the frameworks of NMOFs with extremely high payloads, NMOFs have been a prospective contrast platform for CT. At present, lots of NMOFs with high-Z ions have been obtained and applied as possible CT contrast media. Two NMOFs (Zr-UiO and Hf-UiO) with high loadings of Zr (37 wt%) and Hf (57 wt%) were developed by Lin and co-workers and finally their potential applications as CT contrast agents were demonstrated (Dekrafft et al., 2012). The Zr and Hf NMOFs with corresponding atomic number of 40, 72 respectively making those potential candidates as CT contrast agents. Due to strong X-ray absorbance, Au nanoparticles also could be used as contrast media for CT imaging. Tian groups described an Au nanorod-incorporated core–shell material named Au@MIL-88(Fe), could serve as a multi-mode diagnostic system to provide high resolution image in either MRI or CT imaging by microemulsion method in DMF (Shang et al., 2017). The as-prepared Au@MIL-88(A) nanomaterials in a well-defined star-like morphology structure had high monodispersity and homogeneity. Both CT and MRI induced by Au@MIL-88(Fe) contrast agents showed distinct tumor boundaries with high penetration depth and spatial resolution. Liu groups used IR825 as organic linker to coordinate with Mn^{2+} and Hf^{4+} ions for preparing core-shell NMOFs to act as multi-mode imaging agents (Yang Y et al., 2017). In the NMOF, Mn^{2+} ion are acted as a MRI contrast media; high-Z element Hf^{4+} ion can enhance CT signal and radio-sensitization, and the ligand IR825, is used as a photothermal agent due to the strong NIR absorption.

Positron Emission Tomography (PET). PET is X-ray functional imaging method with superior detection sensitivity (as low as picomolar scope) and stronger signal penetration. In PET, the radionuclides emitted by positrons gather on the target organ, producing a pair of gamma ray photons that can be trapped by sensitive detector panels. Hong and co-workers have done outstanding work on exploring nanomaterial for PET imaging. Recently, they obtained ^{89}Zr-containing NMOF for PET (Chen X et al., 2017). Besides the ^{89}Zr was loading into the framework of UiO-66, the surfaces of the nanomaterial were functionalized by pyrene-derived PEG further. PET scans traced the organ distribution of ^{89}Zr-UiO-66/Py–PGA-PEG-F3 *in vivo* and detected an 8.2 ± 0.3% total injected dose per Gram of tumor after intravenous injection for 2 h.

Optical Imaging. Optical imaging, a kind of fluorescence technique, is widespread in biomedicine. Generally excited dye molecules by visible light in organism and produce luminescence.

FIGURE 10 | (A) Schematic description of the synthesis process of HA conjugated, ICG loading of MIL-100(Fe) nanomaterial. (B) TEM images of the MOF@HA@ICG NPs. (C) FL images (I) and T2-weighted MR images (II) of cells treated with MOF@HA@ICG solutions. (D) FL images of MCF-7 tumor-bearing mice injected with free ICG, MOF@ICG, or MOF@HA@ICG solutions (each with 170 µg/ml of ICG; the tumors are highlighted by red circles). (E) In vitro FL images of organs (heart, liver, kidney, spleen, and lung) and tumors. (F) In vivo PA images and T2-weighted MR images with MOF@HA@ICG treatment. The tumors are highlighted by red circles. Source: (Li et al., 2015).

Highly sensitive and minimally invasive make the optical imaging widely used in clinic.

Recently, by incorporated Yb^{3+} and phenylene-derived photosensitizers, Foucault-Collet and co-workers created unique near-infrared-emitting Yb^{3+}-containing NMOFs (Foucault-Collet et al., 2013). Accompanied by being engulfed by cells and reserved in cytoplasm, Yb^{3+}-based NMOFs emit the number of photons per unit volume that higher enough to realize the real-time imaging of HeLa and NIH 3T3 cells. Li and co-workers constructed core-shell nanomaterial with integrate of single $NaYF_4$: Yb, Er upconversion nanoparticles (UCNPs) into Fe-MIL-101-NH$_2$ to realize luminescent/magnetic dual-mode imaging (Li et al., 2015). The UCNP@Fe-MIL-101-NH$_2$ was further surface-functionalized with PEG and PEG-folic acid (FA) to improve the biocompatibility. A significant KB tumor contrast could be observed after intravenous injection for 24 h in vivo optical imaging. Furthermore, the dyes with optical activity were also inserted within the skeleton of NMOFs either by post synthetically or as an object species to realize the optical imaging. For example, a case of hyaluronic acid (HA) incorporated MIL-100 (Fe) NMOFs were developed by Cai and co-workers (Figures 10A,B). By inserting the indocyanine green (ICG) NIR dye into the NMOFs to realize image-induced PPT [94], this material exhibited a strong load capacity of ICG (40 wt%), high optical stability, and strong NIR absorbance (Figures 10C,D). FL images of the in vivo and in vitro certificated that MOF@HA@ICG had excellent uptake capacity of CD44-positive MCF-7 cells (Figures 10E,F).

CONCLUSION AND OUTLOOK

In the last few years, substantial improvement has been achieved in applying NMOFs for drug delivery, cancer therapy and biomedical sensing and imaging. Various NMOFs-based nanomedicine have been intelligently designed and proved to be effective and powerful for clinic both in vivo and in vitro. In this review, we have comprehensively discussed the update achievements of NMOFs in clinic from a broader vision including applying NMOFs as nanocarriers, anti-cancer therapeutic agents, biosensors and molecular imaging probes as well as well-established synthetic methods for the strengthening their functional capabilities and extending their potential nanomedicine applications. Furthermore, some key issues of NMOFs including controlled synthesis, surface modification, toxicity, biocompatibility, stability, and therapeutic/imaging efficacy before the biomedical applications of NMOFs also are addressed in this review. Despite the sustainable growing interest and impressive accomplishment has been obtained in this area, the development of NMOFs as drug delivery, cancer therapy and biomedical sensing and imaging agents is still in its infancy contrasted to other nanocarriers.

Generally, it can be seen that NMOFs hold obvious superiority compared with other nanoformulations in nanomedicine applications because of their intrinsic characteristics including highly porous and large channels, structural adjustability/

multifunctionality, as well as low toxicity and biocompatibility. Nevertheless, such nanomedical system has boundedness, such as complicated hierarchy for targeted drug delivery without eliminated or undergoes degradation, pure efficiency of phototherapy and photodynamic therapy, difficult fabricating for sensor device and so on. Consequently, there is still defiance in this field and deeper and constant exploration is needed. From a viewpoint of synthetic strategy, one of the biggest challenges is to explore new synthetic methods for the fabrication of smaller-size NMOFs on account of smaller NMOFs has better applicability than larger ones. Still, the smaller NMOFs are better for the integration of biomolecules, particularly in FRET. From the point view of applications, further efforts should be paid to prepare versatile biocompatible and low-toxicity NMOFs. Besides that, chemical instability of NMOFs is essential. Additionally, although lots of researches have proved the short-term safety of NMOFs *in vitro* or *in vivo* studies, the long-term chronic toxicity effects, pathway, and clearance behavior of NMOFs are rarely explored.

In brief, multi-functional NMOFs engineering for nanomedicine is a newly burgeoning field. There is still a large innovative research space in this exciting area. For better applied the NMOFs in disease diagnosis and treatment of clinic application, additional breakthroughs needed to acquire for solving all obstacles mentioned above in the near future.

AUTHOR CONTRIBUTIONS

DZ conceived and wrote the paper; WZ and Z-HW provide partial figures; HX made suggestions to improve the paper.

FUNDING

REFERENCES

Abánades Lázaro, I., and Forgan, R. S. (2019). Application of Zirconium MOFs in Drug Delivery and Biomedicine. *Coord. Chem. Rev.* 380, 230–259. doi:10.1016/j.ccr.2018.09.009

Abánades Lázaro, I., Haddad, S., Sacca, S., Orellana-Tavra, C., Fairen-Jimenez, D., and Forgan, R. S. (2017). Selective Surface PEGylation of UiO-66 Nanoparticles for Enhanced Stability, Cell Uptake, and pH-Responsive Drug Delivery. *Chem* 2 (4), 561–578. doi:10.1016/j.chempr.2017.02.005

Abánades Lázaro, I., Wells, C. J. R., and Forgan, R. S. (2020). Multivariate Modulation of the Zr MOF UiO-66 for Defect-Controlled Combination Anticancer Drug Delivery. *Angew. Chem. Int. Ed.* 59 (13), 5211–5217. doi:10.1002/anie.201915848

Al Haydar, M., Abid, H., Sunderland, B., and Wang, S. (2017). Metal Organic Frameworks as a Drug Delivery System for Flurbiprofen. *Drug Des. Devel Ther.* 11, 2685–2695. doi:10.2147/dddt.s145716

Alexis, F., Pridgen, E., Molnar, L. K., and Farokhzad, O. C. (2008). Factors Affecting the Clearance and Biodistribution of Polymeric Nanoparticles. *Mol. Pharmaceutics* 5 (4), 505–515. doi:10.1021/mp800051m

Amorín-Ferré, L., Busqué, F., Bourdelande, J. L., Ruiz-Molina, D., Hernando, J., and Novio, F. (2013). Encapsulation and Release Mechanisms in Coordination Polymer Nanoparticles. *Chem. Eur. J.* 19 (51), 17508–17516. doi:10.1002/chem.201302662

An, J., Geib, S. J., and Rosi, N. L. (2009). Cation-Triggered Drug Release from a Porous Zinc–Adeninate Metal–Organic Framework. *J. Am. Chem. Soc.* 131 (24), 8376–8377. doi:10.1021/ja902972w

Baa, E., Watkins, G. M., Krause, R. W., and Tantoh, D. N. (2019). Current Trend in Synthesis, Post-Synthetic Modifications and Biological Applications of Nanometal-Organic Frameworks (NMOFs). *Chin. J. Chem.* 37 (4), 378–404. doi:10.1002/cjoc.201800407

Banerjee, S., Lollar, C. T., Xiao, Z., Fang, Y., and Zhou, H.-C. (2020). Biomedical Integration of Metal-Organic Frameworks. *Trends Chem.* 2 (5), 467–479. doi:10.1016/j.trechm.2020.01.007

Bieniek, A., Terzyk, A. P., Wiśniewski, M., Roszek, K., Kowalczyk, P., Sarkisov, L., et al. (2021). MOF Materials as Therapeutic Agents, Drug Carriers, Imaging Agents and Biosensors in Cancer Biomedicine: Recent Advances and Perspectives. *Prog. Mater. Sci.* 117 (23), 100743. doi:10.1016/j.pmatsci.2020.100743

Bůžek, D., Zelenka, J., Ulbrich, P., Ruml, T., Křížová, I., Lang, J., et al. (2017). Nanoscaled Porphyrinic Metal-Organic Frameworks: Photosensitizer Delivery Systems for Photodynamic Therapy. *J. Mater. Chem. B* 5 (9), 1815–1821. doi:10.1039/c6tb03230c

Cai M, M., Chen, G., Qin, L., Qu, C., Dong, X., Ni, J., et al. (2020). Metal Organic Frameworks as Drug Targeting Delivery Vehicles in the Treatment of Cancer. *Pharmaceutics* 12 (3), 232. doi:10.3390/pharmaceutics12030232

Cai X, X., Xie, Z., Li, D., Kassymova, M., Zang, S.-Q., and Jiang, H.-L. (2020). Nano-sized Metal-Organic Frameworks: Synthesis and Applications. *Coord. Chem. Rev.* 417, 213366. doi:10.1016/j.ccr.2020.213366

Cai, W., Chu, C.-C., Liu, G., and Wáng, Y.-X. J. (2015). Metal-Organic Framework-Based Nanomedicine Platforms for Drug Delivery and Molecular Imaging. *Small* 11 (37), 4806–4822. doi:10.1002/smll.201500802

Cai, W., Gao, H., Chu, C., Wang, X., Wang, J., Zhang, P., et al. (2017). Engineering Phototheranostic Nanoscale Metal-Organic Frameworks for Multimodal Imaging-Guided Cancer Therapy. *ACS Appl. Mater. Inter.* 9 (3), 2040–2051. doi:10.1021/acsami.6b11579

Cai, W., Wang, J., Chu, C., Chen, W., Wu, C., and Liu, G. (2019). Metal-Organic Framework-Based Stimuli-Responsive Systems for Drug Delivery. *Adv. Sci.* 6 (1), 1801526. doi:10.1002/advs.201801526

Cao, W., Cui, Y., Yang, Y., and Qian, G. (2021). Dyes Encapsulated Nanoscale Metal-Organic Frameworks for Multimode Temperature Sensing with High Spatial Resolution. *ACS Mater. Lett.* 3 (9), 1426–1432. doi:10.1021/acsmaterialslett.1c00334

Chen, D., Yang, D., Dougherty, C. A., Lu, W., Wu, H., He, X., et al. (2017). *In Vivo* Targeting and Positron Emission Tomography Imaging of Tumor with Intrinsically Radioactive Metal-Organic Frameworks Nanomaterials. *ACS Nano* 11 (4), 4315–4327. doi:10.1021/acsnano.7b01530

Chen, Q., Xu, M., Zheng, W., Xu, T., Deng, H., and Liu, J. (2017). Se/Ru-Decorated Porous Metal-Organic Framework Nanoparticles for the Delivery of Pooled siRNAs to Reversing Multidrug Resistance in Taxol-Resistant Breast Cancer Cells. *ACS Appl. Mater. Inter.* 9 (8), 6712–6724. doi:10.1021/acsami.6b12792

Chen, R., Zhang, J., Chelora, J., Xiong, Y., Kershaw, S. V., Li, K. F., et al. (2017). Ruthenium(II) Complex Incorporated UiO-67 Metal-Organic Framework Nanoparticles for Enhanced Two-Photon Fluorescence Imaging and Photodynamic Cancer Therapy. *ACS Appl. Mater. Inter.* 9 (7), 5699–5708. doi:10.1021/acsami.6b12469

Chen, X., Zhang, M., Li, S., Li, L., Zhang, L., Wang, T., et al. (2017). Facile Synthesis of Polypyrrole@metal-Organic Framework Core-Shell Nanocomposites for Dual-Mode Imaging and Synergistic Chemo-Photothermal Therapy of Cancer Cells. *J. Mater. Chem. B* 5 (9), 1772–1778. doi:10.1039/c6tb03218d

Chen, R., Zhang, J., Wang, Y., Chen, X., Zapien, J. A., and Lee, C.-S. (2015). Graphitic Carbon Nitride Nanosheet@metal-Organic Framework Core-Shell

Nanoparticles for Photo-Chemo Combination Therapy. *Nanoscale* 7 (41), 17299–17305. doi:10.1039/c5nr04436g

Chen, W.-H., Luo, G.-F., Sohn, Y. S., Nechushtai, R., and Willner, I. (2019). Enzyme-Driven Release of Loads from Nucleic Acid-Capped Metal-Organic Framework Nanoparticles. *Adv. Funct. Mater.* 29 (5), 1805341. doi:10.1002/adfm.201805341

Chen W H, W.-H., Luo, G.-F., Vázquez-González, M., Cazelles, R., Sohn, Y. S., Nechushtai, R., et al. (2018). Glucose-Responsive Metal-Organic-Framework Nanoparticles Act as "Smart" Sense-And-Treat Carriers. *ACS Nano* 12 (8), 7538–7545. doi:10.1021/acsnano.8b03417

Chen X, X., Tong, R., Shi, Z., Yang, B., Liu, H., Ding, S., et al. (2018). MOF Nanoparticles with Encapsulated Autophagy Inhibitor in Controlled Drug Delivery System for Antitumor. *ACS Appl. Mater. Inter.* 10 (3), 2328–2337. doi:10.1021/acsami.7b16522

Chen Y, Y., Li, P., Modica, J. A., Drout, R. J., and Farha, O. K. (2018). Acid-Resistant Mesoporous Metal-Organic Framework toward Oral Insulin Delivery: Protein Encapsulation, Protection, and Release. *J. Am. Chem. Soc.* 140 (17), 5678–5681. doi:10.1021/jacs.8b02089

Chen, Y.-A., Tsai, F.-J., Zeng, Y.-T., Wang, J.-C., Hong, C. P., Huang, P.-H., et al. (2016). Fast and Effective Turn-On Paper-Based Phosphorescence Biosensor for Detection of Glucose in Serum. *Jnl Chin. Chem. Soc* 63 (5), 424–431. doi:10.1002/jccs.201500488

Coughlan, C., Ibáñez, M., Dobrozhan, O., Singh, A., Cabot, A., and Ryan, K. M. (2017). Compound Copper Chalcogenide Nanocrystals. *Chem. Rev.* 117 (9), 5865–6109. doi:10.1021/acs.chemrev.6b00376

Cui, R., Zhao, P., Yan, Y., Bao, G., Damirin, A., and Liu, Z. (2021). Outstanding Drug-Loading/Release Capacity of Hollow Fe-Metal-Organic Framework-Based Microcapsules: A Potential Multifunctional Drug-Delivery Platform. *Inorg. Chem.* 60 (3), 1664–1671. doi:10.1021/acs.inorgchem.0c03156

Dekrafft, K. E., Boyle, W. S., Burk, L. M., Zhou, O. Z., and Lin, W. (2012). Zr- and Hf-Based Nanoscale Metal-Organic Frameworks as Contrast Agents for Computed Tomography. *J. Mater. Chem.* 22 (35), 18139–18144. doi:10.1039/c2jm32299d

Deng, J., Wang, K., Wang, M., Yu, P., and Mao, L. (2017). Mitochondria Targeted Nanoscale Zeolitic Imidazole Framework-90 for ATP Imaging in Live Cells. *J. Am. Chem. Soc.* 139 (16), 5877–5882. doi:10.1021/jacs.7b01229

Dong, J., Zhao, D., Lu, Y., and Sun, W.-Y. (2019). Photoluminescent Metal-Organic Frameworks and Their Application for Sensing Biomolecules. *J. Mater. Chem. A.* 7 (40), 22744–22767. doi:10.1039/c9ta07022b

Fang, J. M., Leng, F., Zhao, X. J., Hu, X. L., and Li, Y. F. (2014). Metal-organic Framework MIL-101 as a Low Background Signal Platform for Label-free DNA Detection. *Analyst* 139 (4), 801–806. doi:10.1039/c3an01975f

Foucault-Collet, A., Gogick, K. A., White, K. A., Villette, S., Pallier, A., Collet, G., et al. (2013). Lanthanide Near Infrared Imaging in Living Cells with Yb3+ Nano Metal Organic Frameworks. *Proc. Natl. Acad. Sci.* 110 (43), 17199–17204. doi:10.1073/pnas.1305910110

Fu, G., Liu, W., Feng, S., and Yue, X. (2012). Prussian Blue Nanoparticles Operate as a New Generation of Photothermal Ablation Agents for Cancer Therapy. *Chem. Commun.* 48 (94), 11567–11569. doi:10.1039/c2cc36456e

Hang, L., Zhou, F., Men, D., Li, H., Li, X., Zhang, H., et al. (2017). Functionalized Periodic Au@MOFs Nanoparticle Arrays as Biosensors for Dual-Channel Detection through the Complementary Effect of SPR and Diffraction Peaks. *Nano Res.* 10 (7), 2257–2270. doi:10.1007/s12274-016-1414-1

He, C., Lu, K., and Lin, W. (2014a). Nanoscale Metal-Organic Frameworks for Real-Time Intracellular pH Sensing in Live Cells. *J. Am. Chem. Soc.* 136 (35), 12253–12256. doi:10.1021/ja507333c

He, C., Lu, K., Liu, D., and Lin, W. (2014b). Nanoscale Metal-Organic Frameworks for the Co-delivery of Cisplatin and Pooled siRNAs to Enhance Therapeutic Efficacy in Drug-Resistant Ovarian Cancer Cells. *J. Am. Chem. Soc.* 136 (14), 5181–5184. doi:10.1021/ja4098862

He, Z., Dai, Y., Li, X., Guo, D., Liu, Y., Huang, X., et al. (2019). Hybrid Nanomedicine Fabricated from Photosensitizer-Terminated Metal-Organic Framework Nanoparticles for Photodynamic Therapy and Hypoxia-Activated Cascade Chemotherapy. *Small* 15 (4), 1804131. doi:10.1002/smll.201804131

Horcajada, P., Chalati, T., Serre, C., Gillet, B., Sebrie, C., Baati, T., et al. (2010). Porous Metal-Organic-Framework Nanoscale Carriers as a Potential Platform for Drug Delivery and Imaging. *Nat. Mater* 9, 172–178. doi:10.1038/nmat2608

Horcajada, P., Serre, C., Vallet-Regí, M., Sebban, M., Taulelle, F., and Férey, G. (2006). Metal-Organic Frameworks as Efficient Materials for Drug Delivery. *Angew. Chem.* 118 (118), 6120–6124. doi:10.1002/ange.200601878

Horne, T. K., and Cronjé, M. J. (2017). Mechanistics and Photo-Energetics of Macrocycles and Photodynamic Therapy: An Overview of Aspects to Consider for Research. *Chem. Biol. Drug Des.* 89 (2), 221–242. doi:10.1111/cbdd.12761

Huang, X., El-Sayed, I. H., Qian, W., and El-Sayed, M. A. (2006). Cancer Cell Imaging and Photothermal Therapy in the Near-Infrared Region by Using Gold Nanorods. *J. Am. Chem. Soc.* 128 (6), 2115–2120. doi:10.1021/ja057254a

Illes, B., Hirschle, P., Barnert, S., Cauda, V., Wuttke, S., and Engelke, H. (2017). Exosome-Coated Metal-Organic Framework Nanoparticles: An Efficient Drug Delivery Platform. *Chem. Mater.* 29 (19), 8042–8046. doi:10.1021/acs.chemmater.7b02358

Jeazet, H. B. T., Staudt, C., and Janiak, C. (2012). A Method for Increasing Permeability in O2/N2 Separation with Mixed-Matrix Membranes Made of Water-Stable MIL-101 and Polysulfone. *Chem. Commun.* 48 (15), 2140–2142. doi:10.1039/C2CC16628C

Jiang, K., Zhang, L., Hu, Q., Zhao, D., Xia, T., Lin, W., et al. (2016). Pressure Controlled Drug Release in a Zr-Cluster-Based MOF. *J. Mater. Chem. B* 4 (39), 6398–6401. doi:10.1039/c6tb01756h

Kalra, M. K., Maher, M. M., Toth, T. L., Schmidt, B., Westerman, B. L., Morgan, H. T., et al. (2004). Techniques and Applications of Automatic Tube Current Modulation for CT. *Radiology* 233 (3), 649–657. doi:10.1148/radiol.2333031150

Kato, S., Otake, K.-i., Chen, H., Akpinar, I., Buru, C. T., Islamoglu, T., et al. (2019). Zirconium-Based Metal-Organic Frameworks for the Removal of Protein-Bound Uremic Toxin from Human Serum Albumin. *J. Am. Chem. Soc.* 141 (6), 2568–2576. doi:10.1021/jacs.8b12525

Khoo, V. S., Dearnaley, D. P., Finnigan, D. J., Padhani, A., Tanner, S. F., and Leach, M. O. (1997). Magnetic Resonance Imaging (MRI): Considerations and Applications in Radiotherapy Treatment Planning. *Radiother. Oncol.* 42 (1), 1–15. doi:10.1016/s0167-8140(96)01866-x

Kumar, P., Kumar, P., Bharadwaj, L. M., Paul, A. K., and Deep, A. (2014). Luminescent Nanocrystal Metal Organic Framework Based Biosensor for Molecular Recognition. *Inorg. Chem. Commun.* 43, 114–117. doi:10.1016/j.inoche.2014.02.022

Lan, G., Ni, K., Xu, R., Lu, K., Lin, Z., Chan, C., et al. (2017). Nanoscale Metal-Organic Layers for Deeply Penetrating X-ray-Induced Photodynamic Therapy. *Angew. Chem. Int. Ed.* 56 (40), 12102–12106. doi:10.1002/anie.201704828

Li B B, Wang, X., Chen, L., Zhou, Y., Dang, W., Chang, J., et al. (2018). Ultrathin Cu-TCPP MOF Nanosheets: a New Theragnostic Nanoplatform with Magnetic Resonance/near-Infrared thermal Imaging for Synergistic Phototherapy of Cancers. *Theranostics* 8 (15), 4086–4096. doi:10.7150/thno.25433

Li P, P., Chen, Q., Wang, T. C., Vermeulen, N. A., Mehdi, B. L., Dohnalkova, A., et al. (2018). Hierarchically Engineered Mesoporous Metal-Organic Frameworks toward Cell-free Immobilized Enzyme Systems. *Chem* 4 (5), 1022–1034. doi:10.1016/j.chempr.2018.03.001

Li S Y, S.-Y., Cheng, H., Xie, B.-R., Qiu, W.-X., Zeng, J.-Y., Li, C.-X., et al. (2017). Cancer Cell Membrane Camouflaged cascade Bioreactor for Cancer Targeted Starvation and Photodynamic Therapy. *ACS Nano* 11 (7), 7006–7018. doi:10.1021/acsnano.7b02533

Li W, W., Qi, X., Zhao, C.-Y., Xu, X.-F., Tang, A.-N., and Kong, D.-M. (2017). A Rapid and Facile Detection for Specific Small-Sized Amino Acids Based on Target-Triggered Destruction of Metal Organic Frameworks. *ACS Appl. Mater. Inter.* 9 (1), 236–243. doi:10.1021/acsami.6b13998

Li Y, Y., Li, X., Guan, Q., Zhang, C., Xu, T., Dong, Y., et al. (2017). Strategy for Chemotherapeutic Delivery Using a Nanosized Porous Metal-Organic Framework with a central Composite Design. *Int. J. Nanomedicine* 12, 1465–1474. doi:10.2147/ijn.s119115

Li, S., Tan, L., and Meng, X. (2020). Nanoscale Metal-Organic Frameworks: Synthesis, Biocompatibility, Imaging Applications, and Thermal and Dynamic Therapy of Tumors. *Adv. Funct. Mater.* 30 (13), 1908924. doi:10.1002/adfm.201908924

Li, Y., Tang, J., He, L., Liu, Y., Liu, Y., Chen, C., et al. (2015). Core-Shell Upconversion Nanoparticle@Metal-Organic Framework Nanoprobes for Luminescent/Magnetic Dual-Mode Targeted Imaging. *Adv. Mater.* 27 (27), 4075–4080. doi:10.1002/adma.201501779

Lian, X., Fang, Y., Joseph, E., Wang, Q., Li, J., Banerjee, S., et al. (2017). Enzyme-MOF (Metal-organic Framework) Composites. *Chem. Soc. Rev.* 46 (11), 3386–3401. doi:10.1039/c7cs00058h

Lin, W., Hu, Q., Yu, J., Jiang, K., Yang, Y., Xiang, S., et al. (2016). Low Cytotoxic Metal-Organic Frameworks as Temperature-Responsive Drug Carriers. *ChemPlusChem* 81 (8), 804–810. doi:10.1002/cplu.20160032710.1002/cplu.201600142

Ling, P., Lei, J., Zhang, L., and Ju, H. (2015). Porphyrin-Encapsulated Metal-Organic Frameworks as Mimetic Catalysts for Electrochemical DNA Sensing via Allosteric Switch of Hairpin DNA. *Anal. Chem.* 87 (7), 3957–3963. doi:10.1021/acs.analchem.5b00001

Lismont, M., Dreesen, L., and Wuttke, S. (2017). Metal-organic Framework Nanoparticles in Photodynamic Therapy: Current Status and Perspectives. *Adv. Funct. Mater.* 27 (14), 1606314. doi:10.1002/adfm.201606314

Liu, J., Yang, Y., Zhu, W., Yi, X., Dong, Z., Xu, X., et al. (2016). Nanoscale Metal–organic Frameworks for Combined Photodynamic & Radiation Therapy in Cancer Treatment. *Biomaterials* 97, 1–9. doi:10.1016/j.biomaterials.2016.04.034

Liu, Q., Jin, L.-N., and Sun, W.-Y. (2012). Facile Fabrication and Adsorption Property of a Nano/microporous Coordination Polymer with Controllable Size and Morphology. *Chem. Commun.* 48 (70), 8814–8816. doi:10.1039/c2cc34192a

Liu, W., Wang, Y.-M., Li, Y.-H., Cai, S.-J., Yin, X.-B., He, X.-W., et al. (2017). Fluorescent Imaging-Guided Chemotherapy-And-Photodynamic Dual Therapy with Nanoscale Porphyrin Metal-Organic Framework. *Small* 13 (17), 1603459. doi:10.1002/smll.201603459

Liu, X., Demir, N. K., Wu, Z., and Li, K. (2015). Highly Water-Stable Zirconium Metal-Organic Framework UiO-66 Membranes Supported on Alumina Hollow Fibers for Desalination. *J. Am. Chem. Soc.* 137 (22), 6999–7002. doi:10.1021/jacs.5b02276

Lu, K., Aung, T., Guo, N., Weichselbaum, R., and Lin, W. (2018a). Nanoscale Metal-Organic Frameworks for Therapeutic, Imaging, and Sensing Applications. *Adv. Mater.* 30 (37), 1707634. doi:10.1002/adma.201707634

Lu, K., He, C., Guo, N., Chan, C., Ni, K., Lan, G., et al. (2018b). Low-dose X-ray Radiotherapy–Radiodynamic Therapy via Nanoscale Metal-Organic Frameworks Enhances Checkpoint Blockade Immunotherapy. *Nat. Biomed. Eng.* 2, 600–610. doi:10.1038/s41551-018-0203-4

Lu, K., He, C., Guo, N., Chan, C., Ni, K., Weichselbaum, R. R., et al. (2016). Chlorin-Based Nanoscale Metal-Organic Framework Systemically Rejects Colorectal Cancers via Synergistic Photodynamic Therapy and Checkpoint Blockade Immunotherapy. *J. Am. Chem. Soc.* 138 (38), 12502–12510. doi:10.1021/jacs.6b06663

Lu, Y., Aimetti, A. A., Langer, R., and Gu, Z. (2016). Bioresponsive Materials. *Nat. Rev. Mater.* 2, 16075. doi:10.1038/natrevmats.2016.75

Lu, K., He, C., and Lin, W. (2015). A Chlorin-Based Nanoscale Metal-Organic Framework for Photodynamic Therapy of Colon Cancers. *J. Am. Chem. Soc.* 137 (24), 7600–7603. doi:10.1021/jacs.5b04069

Lu, K., He, C., and Lin, W. (2014). Nanoscale Metal-Organic Framework for Highly Effective Photodynamic Therapy of Resistant Head and Neck Cancer. *J. Am. Chem. Soc.* 136 (48), 16712–16715. doi:10.1021/ja508679h

McKinlay, A. C., Morris, R. E., Horcajada, P., Férey, G., Gref, R., Couvreur, P., et al. (2010). BioMOFs: Metal-Organic Frameworks for Biological and Medical Applications. *Angew. Chem. Int. Edition* 49 (36), 6260–6266. doi:10.1002/anie.201000048

Mejia-Ariza, R., Rosselli, J., Breukers, C., Manicardi, A., Terstappen, L. W. M. M., Corradini, R., et al. (2017). DNA Detection by Flow Cytometry Using PNA-Modified Metal-Organic Framework Particles. *Chem. Eur. J.* 23 (17), 4180–4186. doi:10.1002/chem.201605803

Meng, X., Gui, B., Yuan, D., Zeller, M., and Wang, C. (2016). Mechanized Azobenzene-Functionalized Zirconium Metal-Organic Framework for On-Command Cargo Release. *Sci. Adv.* 2 (8), e1600480. doi:10.1126/sciadv.1600480

Mir, W. J., Sheikh, T., Arfin, H., Xia, Z., Nag, A., Zhang, R., et al. (2020). Lanthanide Doping in Metal Halide Perovskite Nanocrystals: Spectral Shifting, Quantum Cutting and Optoelectronic Applications. *NPG Asia Mater.* 12, 9. doi:10.1038/s41427-019-0192-0

Morris, W., Briley, W. E., Auyeung, E., Cabezas, M. D., and Mirkin, C. A. (2014). Nucleic Acid-Metal Organic Framework (MOF) Nanoparticle Conjugates. *J. Am. Chem. Soc.* 136 (20), 7261–7264. doi:10.1021/ja503215w

Morris, W., Wang, S., Cho, D., Auyeung, E., Li, P., Farha, O. K., et al. (2017). Role of Modulators in Controlling the Colloidal Stability and Polydispersity of the UiO-66 Metal-Organic Framework. *ACS Appl. Mater. Inter.* 9 (39), 33413–33418. doi:10.1021/acsami.7b01040

Nagata, S., Kokado, K., and Sada, K. (2015). Metal-organic Framework Tethering PNIPAM for ON-OFF Controlled Release in Solution. *Chem. Commun.* 51 (41), 8614–8617. doi:10.1039/c5cc02339d

Nazari, M., Rubio-Martinez, M., Tobias, G., Barrio, J. P., Babarao, R., Nazari, F., et al. (2016). Metal-Organic-Framework-Coated Optical Fibers as Light-Triggered Drug Delivery Vehicles. *Adv. Funct. Mater.* 26 (19), 3244–3249. doi:10.1002/adfm.201505260

Nguyen, J. G., Tanabe, K. K., and Cohen, S. M. (2010). Postsynthetic Diazeniumdiolate Formation and NO Release from MOFs. *CrystEngComm* 12 (8), 2335–2338. doi:10.1039/c000154f

Ni, K., Lan, G., Chan, C., Quigley, B., Lu, K., Aung, T., et al. (2018). Nanoscale Metal-Organic Frameworks Enhance Radiotherapy to Potentiate Checkpoint Blockade Immunotherapy. *Nat. Commun.* 9, 2351. doi:10.1038/s41467-018-04703-w

Ni, K., Lan, G., and Lin, W. (2020a). Nanoscale Metal-Organic Frameworks Generate Reactive Oxygen Species for Cancer Therapy. *ACS Cent. Sci.* 6 (6), 861–868. doi:10.1021/acscentsci.0c00397

Ni, K., Luo, T., Nash, G. T., and Lin, W. (2020b). Nanoscale Metal-Organic Frameworks for Cancer Immunotherapy. *Acc. Chem. Res.* 53 (9), 1739–1748. doi:10.1021/acs.accounts.0c00313

Oh, H., Li, T., and An, J. (2015). Drug Release Properties of a Series of Adenine-Based Metal-Organic Frameworks. *Chem. Eur. J.* 21 (47), 17010–17015. doi:10.1002/chem.201501560

Pan, M., Zhu, Y.-X., Wu, K., Chen, L., Hou, Y.-J., Yin, S.-Y., et al. (2017). Epitaxial Growth of Hetero-Ln-MOF Hierarchical Single Crystals for Domain- and Orientation-Controlled Multicolor Luminescence 3D Coding Capability. *Angew. Chem. Int. Ed.* 56 (46), 14582–14586. doi:10.1002/anie.201708802

Park, J., Feng, D., Yuan, S., and Zhou, H. C. (2015). Photochromic Metal-Organic Frameworks: Reversible Control of Singlet Oxygen Generation. *Angew. Chem.* 127 (2), 440–445. doi:10.1002/ange.201408862

Park, J., Jiang, Q., Feng, D., Mao, L., and Zhou, H.-C. (2016a). Size-Controlled Synthesis of Porphyrinic Metal-Organic Framework and Functionalization for Targeted Photodynamic Therapy. *J. Am. Chem. Soc.* 138 (10), 3518–3525. doi:10.1021/jacs.6b00007

Park, J., Jiang, Q., Feng, D., and Zhou, H. C. (2016b). Controlled Generation of Singlet Oxygen in Living Cells with Tunable Ratios of the Photochromic Switch in Metal-Organic Frameworks. *Angew. Chem. Int. Ed.* 55, 7188–7193. doi:10.1002/anie.201602417

Qin, L., Lin, L.-X., Fang, Z.-P., Yang, S.-P., Qiu, G.-H., Chen, J.-X., et al. (2016). A Water-Stable Metal-Organic Framework of a Zwitterionic Carboxylate with Dysprosium: a Sensing Platform for Ebolavirus RNA Sequences. *Chem. Commun.* 52 (1), 132–135. doi:10.1039/c5cc06697b

Ray Chowdhuri, A., Bhattacharya, D., and Sahu, S. K. (2016). Magnetic Nanoscale Metal Organic Frameworks for Potential Targeted Anticancer Drug Delivery, Imaging and as an MRI Contrast Agent. *Dalton Trans.* 45 (7), 2963–2973. doi:10.1039/c5dt03736k

Rieter, W. J., Pott, K. M., Taylor, K. M. L., and Lin, W. (2008). Nanoscale Coordination Polymers for Platinum-Based Anticancer Drug Delivery. *J. Am. Chem. Soc.* 130 (35), 11584–11585. doi:10.1021/ja803383k

Rieter, W. J., Taylor, K. M. L., An, H., Lin, W., and Lin, W. (2006). Nanoscale Metal–Organic Frameworks as Potential Multimodal Contrast Enhancing Agents. *J. Am. Chem. Soc.* 128 (28), 9024–9025. doi:10.1021/ja0627444

Röder, R., Preiß, T., Hirschle, P., Steinborn, B., Zimpel, A., Höhn, M., et al. (2017). Multifunctional Nanoparticles by Coordinative Self-Assembly of His-Tagged Units with Metal-Organic Frameworks. *J. Am. Chem. Soc.* 139 (6), 2359–2368. doi:10.1021/jacs.6b11934

Ruyra, À., Yazdi, A., Espín, J., Carné-Sánchez, A., Roher, N., Lorenzo, J., et al. (2015). Synthesis, Culture Medium Stability, and *In Vitro* and *In Vivo* Zebrafish Embryo Toxicity of Metal-Organic Framework Nanoparticles. *Chem. Eur. J.* 21 (6), 2508–2518. doi:10.1002/chem.201405380

Shang, W., Zeng, C., Du, Y., Hui, H., Liang, X., Chi, C., et al. (2017). Core-Shell Gold Nanorod@Metal-Organic Framework Nanoprobes for Multimodality Diagnosis of Glioma. *Adv. Mater.* 29 (3), 1604381. doi:10.1002/adma.201604381

Sharma, S., Sethi, K., and Roy, I. (2017). Magnetic Nanoscale Metal-Organic Frameworks for Magnetically Aided Drug Delivery and Photodynamic Therapy. *New J. Chem.* 41 (20), 11860–11866. doi:10.1039/c7nj02032e

Simon-Yarza, T., Mielcarek, A., Couvreur, P., and Serre, C. (2018). Nanoparticles of Metal-Organic Frameworks: On the Road to *In Vivo* Efficacy in Biomedicine. *Adv. Mater.* 30 (37), 1707365. doi:10.1002/adma.201707365

Song, L., Li, P.-P., Yang, W., Lin, X.-H., Liang, H., Chen, X.-F., et al. (2018). Low-dose X-ray Activation of W(VI)-doped Persistent Luminescence Nanoparticles for Deep-Tissue Photodynamic Therapy. *Adv. Funct. Mater.* 28 (18), 1707496. doi:10.1002/adfm.2017074910.1002/adfm.201707496

Su, Y. Y., Teng, Z., Yao, H., Wang, S. J., Tian, Y., Zhang, Y. L., et al. (2016). A Multifunctional PB@mSiO2-PEG/DOX Nanoplatform for Combined Photothermal-Chemotherapy of Tumor. *ACS Appl. Mater. Inter.* 8 (27), 17038–17046. doi:10.1021/acsami.6b01147

Sun, Y., Zheng, L., Yang, Y., Qian, X., Fu, T., Li, X., et al. (2020). Metal-Organic Framework Nanocarriers for Drug Delivery in Biomedical Applications. *Nano-micro Lett.* 12, 12. doi:10.1007/s40820-020-00423-3

Tamames-Tabar, C., Cunha, D., Imbuluzqueta, E., Ragon, F., Serre, C., Blanco-Prieto, M. J., et al. (2014). Cytotoxicity of Nanoscaled Metal-Organic Frameworks. *J. Mater. Chem. B* 2 (3), 262–271. doi:10.1039/C3TB20832J

Tan, L.-L., Li, H., Qiu, Y.-C., Chen, D.-X., Wang, X., Pan, R.-Y., et al. (2015). Stimuli-responsive Metal-Organic Frameworks Gated by Pillar[5]arene Supramolecular Switches. *Chem. Sci.* 6 (3), 1640–1644. doi:10.1039/c4sc03749a

Taylor-Pashow, K. M. L., Della Rocca, J., Xie, Z., Tran, S., and Lin, W. (2009). Postsynthetic Modifications of Iron-Carboxylate Nanoscale Metal–Organic Frameworks for Imaging and Drug Delivery. *J. Am. Chem. Soc.* 131 (40), 14261–14263. doi:10.1021/ja906198y

Tian, C., Zhu, L., Lin, F., and Boyes, S. G. (2015). Poly(acrylic Acid) Bridged Gadolinium Metal-Organic Framework-Gold Nanoparticle Composites as Contrast Agents for Computed Tomography and Magnetic Resonance Bimodal Imaging. *ACS Appl. Mater. Inter.* 7 (32), 17765–17775. doi:10.1021/acsami.5b03998

Velásquez-Hernández, M. d. J., Linares-Moreau, M., Astria, E., Carraro, F., Alyami, M. Z., Khashab, N. M., et al. (2021). Towards Applications of bioentities@ MOFs in Biomedicine. *Coord. Chem. Rev.* 429, 213651. doi:10.1016/j.ccr.2020.213651

Wang, B., Lv, X.-L., Feng, D., Xie, L.-H., Zhang, J., Li, M., et al. (2016). Highly Stable Zr(IV)-Based Metal-Organic Frameworks for the Detection and Removal of Antibiotics and Organic Explosives in Water. *J. Am. Chem. Soc.* 138 (19), 6204–6216. doi:10.1021/jacs.6b01663

Wang, D., Zhou, J., Chen, R., Shi, R., Zhao, G., Xia, G., et al. (2016). Controllable Synthesis of Dual-MOFs Nanostructures for pH-Responsive Artemisinin Delivery, Magnetic Resonance and Optical Dual-Model Imaging-Guided Chemo/photothermal Combinational Cancer Therapy. *Biomaterials* 100, 27–40. doi:10.1016/j.biomaterials.2016.05.027

Wang, W., Wang, L., Li, Y., Liu, S., Xie, Z., and Jing, X. (2016a). Nanoscale Polymer Metal-Organic Framework Hybrids for Effective Photothermal Therapy of Colon Cancers. *Adv. Mater.* 28 (42), 9320–9325. doi:10.1002/adma.201602997

Wang, W., Wang, L., Li, Z., and Xie, Z. (2016b). BODIPY-containing Nanoscale Metal-Organic Frameworks for Photodynamic Therapy. *Chem. Commun.* 52 (31), 5402–5405. doi:10.1039/c6cc01048b

Wang Y M, Y.-M., Liu, W., and Yin, X.-B. (2016). Self-limiting Growth Nanoscale Coordination Polymers for Fluorescence and Magnetic Resonance Dual-Modality Imaging. *Adv. Funct. Mater.* 26 (46), 8463–8470. doi:10.1002/adfm.201602925

Wang, C., Volotskova, O., Lu, K., Ahmad, M., Sun, C., Xing, L., et al. (2014). Synergistic Assembly of Heavy Metal Clusters and Luminescent Organic Bridging Ligands in Metal-Organic Frameworks for Highly Efficient X-ray Scintillation. *J. Am. Chem. Soc.* 136 (17), 6171–6174. doi:10.1021/ja500671h

Wang, H.-S., and Wei, J.-P. (2016). Emerging Enantiomeric Resolution Materials with Homochiral Nano-Fabrications. *Nanoscale* 7 (28), 11815–11832. doi:10.1039/c5nr03048j

Wang, S., Chen, Y., Wang, S., Li, P., Mirkin, C. A., and Farha, O. K. (2019). DNA-functionalized Metal-Organic Framework Nanoparticles for Intracellular Delivery of Proteins. *J. Am. Chem. Soc.* 141 (6), 2215–2219. doi:10.1021/jacs.8b12705

Wang, S., McGuirk, C. M., Ross, M. B., Wang, S., Chen, P., Xing, H., et al. (2017). General and Direct Method for Preparing Oligonucleotide-Functionalized Metal-Organic Framework Nanoparticles. *J. Am. Chem. Soc.* 139 (29), 9827–9830. doi:10.1021/jacs.7b05633

Wang, S., Morris, W., Liu, Y., McGuirk, C. M., Zhou, Y., Hupp, J. T., et al. (2015). Surface-Specific Functionalization of Nanoscale Metal-Organic Frameworks. *Angew. Chem.* 127 (127), 14951–14955. doi:10.1002/ange.201506888

Wen, T., Quan, G., Niu, B., Zhou, Y., Zhao, Y., Lu, C., et al. (2021). Versatile Nanoscale Metal-Organic Frameworks (nMOFs): An Emerging 3D Nanoplatform for Drug Delivery and Therapeutic Applications. *Small* 17 (8), 2005064. doi:10.1002/smll.202005064

Wu, M.-X., and Yang, Y.-W. (2017). Metal-Organic Framework (MOF)-Based Drug/Cargo Delivery and Cancer Therapy. *Adv. Mater.* 29 (23), 1606134. doi:10.1002/adma.201606134

Wu, Q., Niu, M., Chen, X., Tan, L., Fu, C., Ren, X., et al. (2018). Biocompatible and Biodegradable Zeolitic Imidazolate Framework/polydopamine Nanocarriers for Dual Stimulus Triggered Tumor Thermo-Chemotherapy. *Biomaterials* 162, 132–143. doi:10.1016/j.biomaterials.2018.02.022

Wuttke, S., Braig, S., Preiß, T., Zimpel, A., Sicklinger, J., Bellomo, C., et al. (2015). MOF Nanoparticles Coated by Lipid Bilayers and Their Uptake by Cancer Cells. *Chem. Commun.* 51 (87), 15752–15755. doi:10.1039/C5CC06767G

Xu, M., Yuan, S., Chen, X.-Y., Chang, Y.-J., Day, G., Gu, Z.-Y., et al. (2017). Two-Dimensional Metal-Organic Framework Nanosheets as an Enzyme Inhibitor: Modulation of the α-Chymotrypsin Activity. *J. Am. Chem. Soc.* 139 (24), 8312–8319. doi:10.1021/jacs.7b03450

Xu, R., Wang, Y., Duan, X., Lu, K., Micheroni, D., Hu, A., et al. (2016). Nanoscale Metal-Organic Frameworks for Ratiometric Oxygen Sensing in Live Cells. *J. Am. Chem. Soc.* 138 (7), 2158–2161. doi:10.1021/jacs.5b13458

Yang, B., Chen, Y., and Shi, J. (2019). Reactive Oxygen Species (ROS)-based Nanomedicine. *Chem. Rev.* 119 (8), 4881–4985. doi:10.1021/acs.chemrev.8b00626

Yang, X., Tang, Q., Jiang, Y., Zhang, M., Wang, M., and Mao, L. (2019). Nanoscale ATP-Responsive Zeolitic Imidazole Framework-90 as a General Platform for Cytosolic Protein Delivery and Genome Editing. *J. Am. Chem. Soc.* 141 (9), 3782–3786. doi:10.1021/jacs.8b11996

Yang, J., Grzech, A., MulderDingemans, F. M. T. J., and Dingemans, T. J. (2011). Methyl Modified MOF-5: a Water Stable Hydrogen Storage Material. *Chem. Commun.* 47 (18), 5244–5246. doi:10.1039/C1CC11054C

Yang, S.-P., Chen, S.-R., Liu, S.-W., Tang, X.-Y., Qin, L., Qiu, G.-H., et al. (2015). Platforms Formed from a Three-Dimensional Cu-Based Zwitterionic Metal-Organic Framework and Probe Ss-DNA: Selective Fluorescent Biosensors for Human Immunodeficiency Virus 1 Ds-DNA and Sudan Virus RNA Sequences. *Anal. Chem.* 87 (24), 12206–12214. doi:10.1021/acs.analchem.5b03084

Yang, S.-P., Zhao, W., Hu, P.-P., Wu, K.-Y., Jiang, Z.-H., Bai, L.-P., et al. (2017). Lanthanum-Based Metal-Organic Frameworks for Specific Detection of Sudan Virus RNA Conservative Sequences Down to Single-Base Mismatch. *Inorg. Chem.* 56 (24), 14880–14887. doi:10.1021/acs.inorgchem.7b02107

Yang, Y., Chao, Y., Liu, J., Dong, Z., He, W., Zhang, R., et al. (2017). Core-shell and Co-doped Nanoscale Metal-Organic Particles (NMOPs) Obtained via post-synthesis Cation Exchange for Multimodal Imaging and Synergistic Thermo-Radiotherapy. *NPG Asia Mater.* 9, e344. doi:10.1038/am.2016.205

Yang, X., Gao, L., Guo, Q., Li, Y., Ma, Y., Yang, J., et al. (2020). Nanomaterials for Radiotherapeutics-Based Multimodal Synergistic Cancer Therapy. *Nano Res.* 13, 2579–2594. doi:10.1007/s12274-020-2722-z

Yang, Y., Liu, J., Liang, C., Feng, L., Fu, T., Dong, Z., et al. (2016). Nanoscale Metal-Organic Particles with Rapid Clearance for Magnetic Resonance Imaging-Guided Photothermal Therapy. *ACS Nano* 10 (2), 2774–2781. doi:10.1021/acsnano.5b07882

Yin, H.-Q., Yang, J.-C., and Yin, X.-B. (2017). Ratiometric Fluorescence Sensing and Real-Time Detection of Water in Organic Solvents with One-Pot Synthesis of Ru@MIL-101(Al)-NH2. *Anal. Chem.* 89 (24), 13434–13440. doi:10.1021/acs.analchem.7b03723

Zhang, Q., Lei, M., Kong, F., and Yang, Y. (2018). A Water-Stable Homochiral Luminescent MOF Constructed from an Achiral Acylamide-Containing Dicarboxylate Ligand for Enantioselective Sensing of Penicillamine. *Chem. Commun.* 54 (77), 10901–10904. doi:10.1039/c8cc06274a

Zhang, W., Li, S., Liu, X., Yang, C., Hu, N., Dou, L., et al. (2018). Oxygen-Generating MnO2 Nanodots-Anchored Versatile Nanoplatform for Combined

Chemo-Photodynamic Therapy in Hypoxic Cancer. *Adv. Funct. Mater.* 28 (13), 1706375. doi:10.1002/adfm.201706375

Zhang, Y., Fu, H., Chen, S., Liu, B., Sun, W., and Gao, H. (2020). Construction of an Iridium(iii)-Complex-Loaded MOF Nanoplatform Mediated with a Dual-Responsive Polycationic Polymer for Photodynamic Therapy and Cell Imaging. *Chem. Commun.* 56 (5), 762–765. doi:10.1039/C9CC09357E

Zhao, D., Liu, X.-H., Guo, J.-H., Xu, H.-J., Zhao, Y., Lu, Y., et al. (2018). Porous Metal-Organic Frameworks with Chelating Multiamine Sites for Selective Adsorption and Chemical Conversion of Carbon Dioxide. *Inorg. Chem.* 57 (5), 2695–2704. doi:10.1021/acs.inorgchem.7b03099

Zhao, D., Liu, X.-H., Zhao, Y., Wang, P., Liu, Y., Azam, M., et al. (2017). Luminescent Cd(ii)-Organic Frameworks with Chelating NH2 Sites for Selective Detection of Fe(iii) and Antibiotics. *J. Mater. Chem. A.* 5 (30), 15797–15807. doi:10.1039/c7ta03849f

Zhao, H.-Q., Qiu, G.-H., Liang, Z., Li, M.-M., Sun, B., Qin, L., et al. (2016a). A Zinc(II)-based Two-Dimensional MOF for Sensitive and Selective Sensing of HIV-1 Ds-DNA Sequences. *Analytica Chim. Acta* 922, 55–63. doi:10.1016/j.aca.2016.03.054

Zhao, H.-Q., Yang, S.-P., Ding, N.-N., Qin, L., Qiu, G.-H., Chen, J.-X., et al. (2016b). A Zwitterionic 1D/2D Polymer Co-crystal and its Polymorphic Sub-components: a Highly Selective Sensing Platform for HIV Ds-DNA Sequences. *Dalton Trans.* 45 (12), 5092–5100. doi:10.1039/C5DT04410C

Zhao, H.-X., Zou, Q., Sun, S.-K., Yu, C., Zhang, X., Li, R.-J., et al. (2016). Theranostic Metal-Organic Framework Core-Shell Composites for Magnetic Resonance Imaging and Drug Delivery. *Chem. Sci.* 7 (8), 5294–5301. doi:10.1039/c6sc01359g

Zhao, S.-N., Wu, L.-L., Feng, J., Song, S.-Y., and Zhang, H.-J. (2016). An Ideal Detector Composed of a 3D Gd-Based Coordination Polymer for DNA and Hg2+ Ion. *Inorg. Chem. Front.* 3 (3), 376–380. doi:10.1039/c5qi00252d

Zhao, J., Yin, F., Ji, L., Wang, C., Shi, C., Liu, X., et al. (2020). Development of a Tau-Targeted Drug Delivery System Using a Multifunctional Nanoscale Metal-Organic Framework for Alzheimer's Disease Therapy. *ACS Appl. Mater. Inter.* 12 (40), 44447–44458. doi:10.1021/acsami.0c11064

Zheng, H., Zhang, Y., Liu, L., Wan, W., Guo, P., Nyström, A. M., et al. (2016). One-pot Synthesis of Metal-Organic Frameworks with Encapsulated Target Molecules and Their Applications for Controlled Drug Delivery. *J. Am. Chem. Soc.* 138 (3), 962–968. doi:10.1021/jacs.5b11720

Zhou, J., Tian, G., Zeng, L., Song, X., and Bian, X.-w. (2018). Nanoscaled Metal-Organic Frameworks for Biosensing, Imaging, and Cancer Therapy. *Adv. Healthc. Mater.* 7 (10), 1800022. doi:10.1002/adhm.201800022

Zhu, W., Xiang, G., Shang, J., Guo, J., Motevalli, B., Durfee, P., et al. (2018). Versatile Surface Functionalization of Metal-Organic Frameworks through Direct Metal Coordination with a Phenolic Lipid Enables Diverse Applications. *Adv. Funct. Mater.* 28 (16), 1705274. doi:10.1002/adfm.201705274

Zhu, X.-D., Zhang, K., Wang, Y., Long, W.-W., Sa, R.-J., Liu, T.-F., et al. (2018). Fluorescent Metal-Organic Framework (MOF) as a Highly Sensitive and Quickly Responsive Chemical Sensor for the Detection of Antibiotics in Simulated Wastewater. *Inorg. Chem.* 57 (3), 1060–1065. doi:10.1021/acs.inorgchem.7b02471

Zhu, X., Zheng, H., Wei, X., Lin, Z., Guo, L., Qiu, B., et al. (2013). Metal-organic Framework (MOF): a Novel Sensing Platform for Biomolecules. *Chem. Commun.* 49 (13), 1276–1278. doi:10.1039/c2cc36661d